MSc Program
Renewable Energy Systems

Comparison between Green and Blue Hydrogen Production: Climate Impact, Status Quo and Prospects.

A Master's Thesis submitted for the degree of
"Master of Science"

supervised by
Ao.Univ.Prof. Dipl.-Ing. Dr.techn. Michael Harasek

Oscar Ivan Barbosa Aguas, BSc

11946199

Vienna, 05.02.2023

Affidavit

I, **OSCAR IVAN BARBOSA AGUAS, BSC**, hereby declare

1. that I am the sole author of the present Master's Thesis, "COMPARISON BETWEEN GREEN AND BLUE HYDROGEN PRODUCTION: CLIMATE IMPACT, STATUS QUO AND PROSPECTS.", 91 pages, bound, and that I have not used any source or tool other than those referenced or any other illicit aid or tool, and
2. that I have not prior to this date submitted the topic of this Master's Thesis or parts of it in any form for assessment as an examination paper, either in Austria or abroad.

Vienna, 05.02.2023

____
Signature

Abstract

Blue and green hydrogen are considered low-carbon technologies and important players in decarbonizing the energy sector and tackling $CO_{2\text{-eq}}$ emissions. However, hydrogen production is currently dominated by fossil fuels (gas, oil, and coal), which are known as gray, black, or brown hydrogen. Gray hydrogen is converted to blue when it is coupled with CCUS to capture and store CO_2 emissions. On the other hand, green hydrogen comes from electrolysis using renewable electricity from wind and solar PV, among others. A literature review of gray, blue, and green hydrogen production technologies is carried out. The results of the literature review show that blue hydrogen production does not capture all CO_2 emissions, capture efficiencies vary depending on the selected technology, and methane leakage rates during production and transport are significant. Green hydrogen has the lowest climate impact because there is no direct use of fossil fuels. However, its deployment is still in development. In this thesis, a comparative analysis of the climate impact of the estimated hydrogen demand for 2030 and 2050 was conducted according to the future shares of gray, blue, and green hydrogen using calculated carbon intensities ($CO_{2\text{-eq}}/kgH_2$). Results show that i) there is a significant reduction of emissions when the share of gray hydrogen is overcome by blue and green hydrogen in every scenario; ii) comparing the results with previously estimated emissions for 2020 and 2030, it can be seen that previous $CO_{2\text{-eq}}$ emissions were underestimated; iii) only for the 100% green hydrogen scenario, emissions were close to or under the $CO_{2\text{-eq}}$ emissions of 2020. It is important to note that the data used for the comparative analysis are estimates and do not correspond to what is currently achieved in terms of efficiency, carbon capture rate, and methane leakage. In conclusion, under current technological conditions, green hydrogen is the least carbon-intensive option compared to blue and gray hydrogen, and its share in the hydrogen mix should be prioritized. However, the carbon intensity of green hydrogen depends on the adopted renewable energy source.

Table of content

1 Introduction

The twenty-first century is marked by ongoing and drastically developing climate change. Climate change refers to alterations in the climatic conditions that currently proliferate faster than expected on our planet Earth. Climate change is correlated with the increase in global average temperature levels (Kumar et al., 2021, pp. 1–2), which hit roughly 1°C above pre-industrial levels in 2017 (IPCC, 2022). Global warming refers to that increase in temperature due to the rise of greenhouse gases such as carbon dioxide (CO_2), methane (CH_4), nitrous oxide (N_2O), and water (moisture) in the atmosphere (Kumar et al., 2021, pp. 1–2).

For the 21st century, the temperature increase is anticipated to range between 1.8 and 4°C (Kumar et al., 2021, p. 1). 2021 was already one of the sixth warmest years since the end of the 19th century (NASA, 2022). An average temperature rise of 2°C already has drastic consequences for humanity and nature. Extreme weather events, droughts, and food scarcity give a glimpse of the severity of climate change and its interconnectedness with other crises. In addition, rising sea levels and melting glaciers reveal substantial consequences for our ecosystem. Climate change is human-made and was radically boosted by the industrial revolution and the consumption of fossil fuel resources (IPCC, 2022).

Greenhouse gases are naturally present in the lower atmosphere, where they retain heat, leading to the greenhouse effect and the warming of the earth's surface. This process is essential for supporting life on the planet as, without it, temperatures would drop to about -18°C. Therefore, the abundance of greenhouse gases in the atmosphere determines the greenhouse effect intensity (Yoro & Daramola, 2020, pp. 9–10).

Researchers have noted that CO_2, SO_2, CH_4, and N_2O are the four principal greenhouse gases that receive significant attention from scholars worldwide (Yoro & Daramola, 2020, p. 10). Anthropogenic CO_2 emissions come mainly from fossil fuel combustion for energy and transport. Moreover, deforestation and chemical reactions in the industrial sectors, such as cement production, cause the majority of CO_2 emissions into the atmosphere (Yoro & Daramola, 2020, pp. 8-9). According to Table 1 (Yoro & Daramola, 2020, p. 11), the use of fossil fuels was responsible for more than 83% of greenhouse gas emissions in 2019.

Table 1. Greenhouse gases and their significant sources (Yoro & Daramola, 2020, p. 11).[1]

Greenhouse gases	Sources	% Emission in 2019
Carbon dioxide (CO_2)	Fossil fuel combustion, deforestation	76
Methane (CH_4)	Biomass combustion, agricultural wastes	13
Nitrous oxide (N_2O)	Fertilizer use	3
Sulfur dioxide (SO_2)	Combustion of coal, oil, and diesel	7
Fluorinated gases (CFCs, HCFs)	Refrigeration	1

Methane (CH_4) concentration in the atmosphere has increased mainly because of emissions from the energy sector, followed by the agricultural industry and landfills. Its warming potential (GWP) over 100 years is 28-36 times larger than the GWP of CO_2, placing methane as the second most emitted anthropogenic gas (Yoro & Daramola, 2020, p. 7).

Nitrous oxide (N_2O) is in third place as it is a greenhouse gas with a high warming potential. The GWP effects of nitrous oxide over a period of 100 years are greater than those from carbon dioxide and methane. In nature, the sources of N_2O are soil, tundra, and the oceans. Significant anthropogenic emissions come from agriculture, such as animal waste, combustion of biomass, and the fertilizer industry. The primary anthropogenic source of N_2O is fertilizers used for nitrogen enrichment of the soil. Moreover, the processes involved in biogas production highly contribute to N_2O emissions (Yoro & Daramola, 2020, p. 8).

Fluorinated gases (F-gases) are entirely anthropogenic with a high GWP of around 140 to 23,500 times more than carbon dioxide and are classified as 'super-pollutants'. There are four different F-gases: HFCs, PFCs, SF6, and NF3. Hydrofluorocarbons (HFCs) are mainly used as coolants in freezers and air conditioning. Perfluorocarbons (PFCs) are employed in the production of electronics, such as solar panels and plasma cleaning of semiconductors. The aluminum industry is a significant source of PFCs. The strongest greenhouse gas ever identified is Sulfur hexafluoride (SF6), used by the electricity industry in transmission lines and distribution grids. NF3, or nitrogen trifluoride, is an etching agent used in silicon wafer production and electronics (Sovacool et al., 2021, pp. 1–2)

[1] Reprinted from Advances in Carbon Capture, Kelvin O. Yoro, Michael O. Daramola, Chapter 1 CO2 emission sources, greenhouse gases, and the global warming effect, 3-28, Copyright (2020), with permission from Elsevier.

Sulfur dioxide (SO_2) is emitted when burning fossil fuels. The main sources of SO_2 are power plants, followed by the metal industry, ships, heavy trucks, and volcanoes (natural sources) (Yoro & Daramola, 2020, p. 9). It is not considered a greenhouse gas (Johnston et al., 2008, p. 748). However, SO_2 reacts with other airborne contaminants to produce sulfate particles. These particles are components of particulate matter (PM2.5) which are associated with health problems due to inhalation and exposure. In addition, a combination of SO_2 and nitrogen oxides (NOx) results in acid rain affecting visibility and harming the environment (Yoro & Daramola, 2020, p. 9).

In terms of greenhouse gas emissions by sector, these are classified into five categories. First, the energy systems represented 34% of total emissions in 2018, in which electricity generation by coal combustion plays an important role. Followed by industry supplying basic materials such as chemicals, metals, and cement. Third, agriculture, forestry, and other land use (AFOLU) are directly linked to essential services like food and wood production. Finally, transport and building represent 20% and are connected to cities, infrastructure, and people's behavior. Figure 1 shows the global GHG emissions trend from 1990 to 2018. It can be seen that emissions have increased gradually (Lamb et al., 2021).

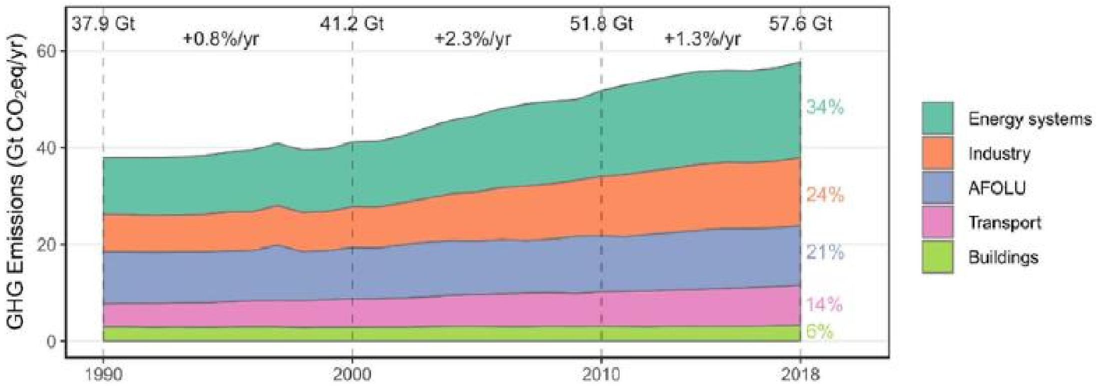

Figure 1. Total global GHG emissions trends by sector (Lamb et al., 2021, p. 6).

After numerous calls to take action to curb global warming effects, 196 countries, including the European Union, met in Paris in 2015 with the aim of agreeing on a global temperature target. As a result, for the first time in history, a legally binding global treaty on climate change accepted by all countries was signed. Participants committed to maintaining global warming to 2 degrees, if possible, to 1.5 degrees Celsius and to accomplish carbon neutrality by 2050. The agreement calls for countries to take immediate climate action over a five-year period. At the end of each period, mandatory Nationally Determined Contributions (NDCs) are submitted by each nation to address climate change. Furthermore, long-term strategies (LT-LEDS) are a voluntary addition that encourages countries to develop the NDCs into long-term goals (UNFCCC, 2022).

The agreement emphasizes collaboration between countries through a financial, technological, and capacity-building support framework. It encourages developed countries to take the lead in supporting countries where needed to achieve climate change goals. The framework highlights the importance of assisting vulnerable countries in developing capacity-building actions related to the climate. It also provides financial support for large-scale investments in mitigating GHG and adapting to adverse effects caused by increases in global temperatures. The technology framework similarly adopts a Technology Mechanism to accelerate its development and transfer (UNFCCC, 2022).

Due to the pressure from climate change and the international agreement on an energy transition, energy production needs to be decarbonized. Hydrogen (H_2) is considered a key player in decarbonizing the energy sector worldwide; however, companies, organizations, and governments take different approaches to be the first in the energy transition to tackle climate change.

This thesis focuses on hydrogen and its potential for a green energy transition analyzing its $CO_{2\text{-eq}}$ emissions. Therefore, a literature analysis is made to illustrate the current state of blue and green hydrogen technology's development. Moreover, the $CO_{2\text{-eq}}$ emissions per kg H_2 ($kgCO_{2\text{-eq}}/kgH_2$) and the current and future hydrogen demand in a million tons (Mt) are taken from reports and peer review papers. Finally, a calculation was made to compare the $CO_{2\text{-eq}}$ emissions from gray, blue, and green hydrogen in 2020, 2030 (short term), and 2050 (long term). Results will show how this is aligned with the target of reducing CO_2 emissions and keeping global temperatures below 1.5^0C.

2 Hydrogen Technology

Hydrogen has been used for over 200 years. Its long history goes back to the 19th century when internal combustion engines ran on hydrogen for the first time. From the following centuries to the present day, it has helped lift air balloons, propel rockets to the moon, and feed the rapid population growth with ammonia, an essential element in fertilizer production (IEA, 2019).

It is gaining recognition due to its high energy content, high conversion efficiency, potential for storage, and the benefit of being a clean fuel when produced from renewable electricity (Espegren et al., 2021).

2.1. Definition of Hydrogen

Hydrogen, the central compound of sequence stars, can be found within the universe as the most abundant element. It is displayed with the atomic number 1 as the first element, next to the alkali metals on the left side of the periodic table. Although, it is not part of the alkali metals group, this nonmetal element is unique in its class. Hydrogen is found in three different isotopes; protium, the most abundant, contains one proton in its nucleus, followed by deuterium, with one proton and one neutron, and tritium, with one proton and two neutrons being the only radioactive one among the three (Zohuri, 2019). Hydrogen's importance comes, for instance, when it reacts with carbon to produce a tremendous assortment of natural particles known as hydrocarbons and, with oxygen, to become water, the most significant compound on the planet (Basile et al., 2015).

In nature, Hydrogen exits as a gas in its molecular form, 'H_2'. It is a very flammable gas with no taste, color or odor. When reaching a temperature of -252^{0}C, it becomes liquid (condensation point), and not far from it, at a temperature of -259^{0}C, it becomes solid (solidification point) (Basile et al., 2015), with an atomic weight of 1.008, it is considered the lightest element (Zohuri, 2019). Table 2 summarizes the physical properties of hydrogen and compares them to standard fuels.

Table 2. Physical properties of hydrogen (IEA, 2019, p. 35).

Property	Hydrogen	Comparison
Density (gaseous)	0.089 kg/m^3 (0 °C, 1 bar)	1/10 of natural gas
Density (liquid)	70.79 kg/m^3 (-253 °C, 1 bar)	1/6 of natural gas
Boiling point	-252.76 °C (1 bar)	90 °C below LNG
Energy per unit of mass (LHV)	120.1 MJ/kg	3x that of gasoline
Energy density (ambient cond., LHV)	0.01 MJ/kg	1/3 of natural gas

Specific energy (liquefied, LHV)	8.5 MJ/kg	1/3 of LNG
Flame velocity	346 cm/s	8x methane
Ignition range	4-77 % in the air by volume	6x wider than methane
Auto ignition temperature	585 °C	220 °C for gasoline
Ignition energy	0.02 MJ	1/10 of methane
Notes: cm/s= centimeter per second; kg/m^3= kilograms per cubic meter; LHV= lower heating value; MJ= megajoule; MJ/kg= megajoule per kilogram; MJ/L= megajoule per liter.		

In terms of energy content per mass, hydrogen has a value of 143 MJ/kg when combusted. It is three times higher than liquid fuels, such as gasoline or biodiesel, and almost three times higher than natural gas. Nevertheless, when talking about volumetric energy density, hydrogen has the lowest value, with 0.0107 MJ/L at ambient pressure, when compared with natural gas under the same conditions, making it necessary to compress it to improve the energy content per volume, as shown in Table 3 (Mazloomi & Gomes, 2012, p. 3025).

Table 3. Volumetric and gravimetric energy densities of standard fuels. Compiled by author from Engineering ToolBox (2003); Mazloomi & Gomes (2012, p. 3025).

Material	Energy LHV (MJ/kg)	Energy HHV (MJ/kg)	Energy per Liter (MJ/l)
Hydrogen (liquid)	120	143	10.1
Hydrogen (compressed, 700 bar)	120	143	5.6
Hydrogen (ambient pressure)	120	143	0.0107
Methane (ambient pressure)	50	55.6	0.0378
Natural gas (liquid)	47.1*	53.6	22.2
Natural gas (compressed, 250 bar)	47.1*	53.6	9
Natural gas	47.1*	53.6	0.0364
LPG propane	45.5*	49.6	25.3
LPG butane	45.5*	49.1	27.7
Gasoline (petrol)	43.4*	46.4	34.2
Biodiesel oil	37.8*	42.2	33
Diesel	42.6*	45.4	34.6
**** The quality of fuels, a blend of various components, can change with the seasons and markets. For fuels with the specified density, the values are provided. The quality variance may result in heating levels that are 5% to 10% higher or lower than the stated value.***			

The Higher Heating Value (HHV) considers the energy needed to vaporize water produced during combustion. In contrast, the Lower Heating Value (LHV) does not include this amount of energy, which is lost and cannot be recovered after combustion (Admin, 2019).

2.2. Global Hydrogen Demand

In 2020, estimates of hydrogen demand worldwide were about 90 Mt H_2. Figure 2 shows the growth in hydrogen demand, which almost doubled from 2000 to 2020 in different sectors (IEA, 2021a).

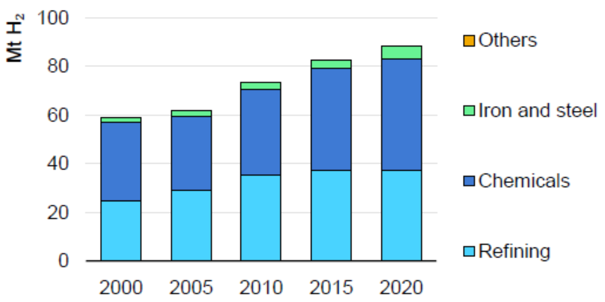

Figure 2. Hydrogen demand by sector 2000-2020 (IEA, 2021a, p. 43).

Hydrogen consumption in oil refineries (the single largest user) accounted for nearly 40 Mt H_2, mainly to eliminate sulfur and to obtain light hydrocarbon products from heavy oil. Most hydrogen is supplied as a by-product from naphtha reforming and petrochemical processes inside the refinery. At the same time, the remainder comes from external sources or onsite production from natural gas reforming and, to a minor extent, coal gasification (IEA, 2021a).

The chemical subsector used 46 Mt H_2 as a feedstock in the industry to produce mainly ammonia and methanol. In this industry, ammonia production is the biggest hydrogen consumer, with 33 Mt H_2 of total consumption. It has industrial uses in fertilizers, synthetic fibers, explosives, and other specialized materials. Methanol production accounted for 13 Mt H_2. Formaldehyde is the most common product for industrial uses, although numerous fuel uses, immediately or after conversion, are also significant (IEA, 2021a).

The last subsector in the industry is the manufacturing of iron and steel. It consumed around 5 Mt H_2 in 20202 to reduce iron ore into Direct Reduced Iron (DRI). In this process, hydrogen and carbon monoxide work together as a synthesis gas, forming a mixture with usually 0 to 70% of hydrogen (IEA, 2021a). Figure 3 summarizes hydrogen demand in the industry in 2020.

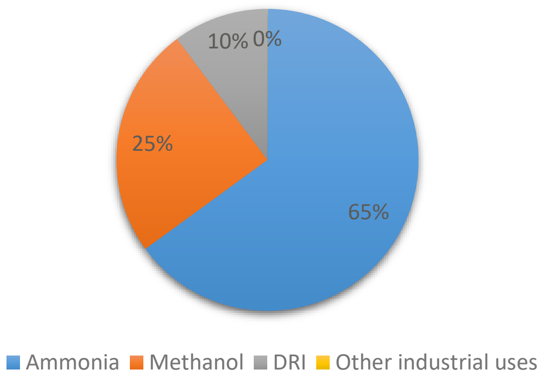

Figure 3. Global Hydrogen demand in industry, 2020 (IEA, 2021a, p. 55).

2.3. Hydrogen Production

Despite hydrogen being the most abundant element in the universe, it is always found in conjunction with other elements making it necessary to separate it. As such, hydrogen can be produced from renewable and non-renewable resources (Arat & Sürer, 2018). However, 96% of current hydrogen production comes from non-renewable resources, with steam-methane reforming (SMR) being the most common method, followed by coal and oil gasification. On the other hand, renewable hydrogen via water electrolysis and other sources accounts just for 4% of total production (Figure 4) (IRENA, 2018).

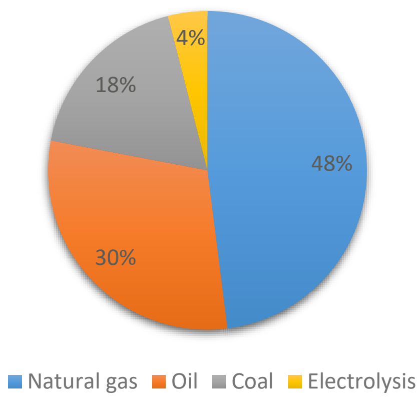

Figure 4. Hydrogen production sources (IRENA, 2018, p. 14).

Figure 5 below gives an overview of the different production methods to obtain hydrogen from renewable and non-renewable sources available today. It can be seen that hydrogen can be produced not only via water electrolysis and steam methane reforming of natural gas (SMR) but from more technologies within the two categories.

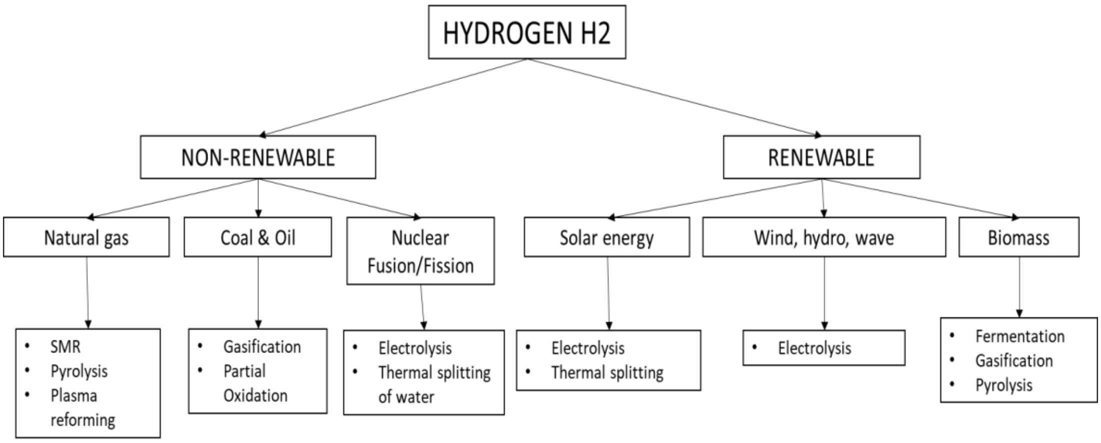

Figure 5. Hydrogen production methods. Own figure based on Arat & Sürer (2018, p. 22).

2.4. Hydrogen Classification by Colors

Colors are increasingly being used to describe the various processes and sources of hydrogen production in recent years. However, because not all conditions for hydrogen production fall into a single-color classification, policies should be based on the lifecycle of GHG emissions and their impact. Gray, Blue, Green, and Turquoise (Figure 6), are the most well-known colors today and will be discussed further below. (IRENA, 2020a):

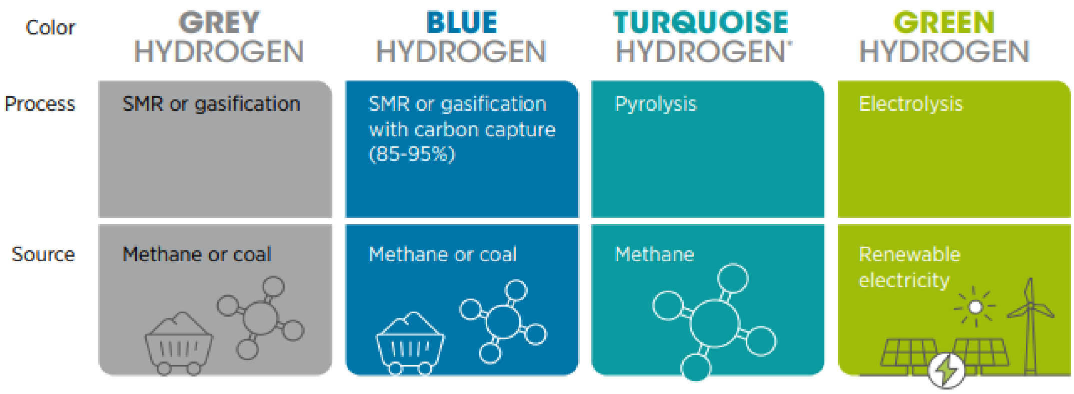

Figure 6. Hydrogen classification by colors (IRENA, 2020a, p. 8).

- **Gray hydrogen**: This is sometimes referred to as Black or Brown, and it comes from fossil fuels via SMR or coal gasification. When produced, considerable amounts of CO_2 are emitted into the atmosphere, making these technologies unsuitable for a net-zero emissions path (IRENA, 2020a).

- **Blue hydrogen**: Gray, Black, or Brown hydrogen production is used along with carbon capture and storage (CCS) to capture CO_2 and reduce its emission into the atmosphere. However, the deployment of this technology has limitations as efficiencies are expected to reach between 85 to 95% while continuing to rely on finite resources (natural gas, oil, coal) affected by fluctuating prices. This means CO_2 emissions will still be between 5 to 15%. Therefore, this technology is considered a short-term solution for use in the energy transition (IRENA, 2020a).

- **Turquoise hydrogen**: Currently still in the R&D stage. Turquoise hydrogen is produced from natural gas with no CO_2 emissions and solid carbon as a byproduct, which can be stored more easily than gaseous CO_2 (IRENA, 2020a).

- **Green hydrogen**: Hydrogen produced commercially (IRENA, 2020a) with nearly no CO_2 emissions (Gonzalez-Diaz et al., 2021, p. 1). The process consists of using water electrolysis and renewable electricity (i.e., from wind turbines and solar PV, among others). The method has been gaining interest due to the low cost of variable renewable energy (VRE) and technology development, which have reduced overall costs for the production of green hydrogen (IRENA, 2020a).

According to the classifications above, gray hydrogen is obtained via hydrocarbon reforming, while low-emission hydrogen derives from blue and green technologies. Thus, for this thesis, only H_2 production from hydrocarbon reforming (natural gas, oil, and carbon) coupled with CCS and H_2 production from water electrolysis via renewable electricity (wind and solar) will be considered.

2.5. Hydrocarbon Reforming

Gray hydrogen (sometimes referred to as black or brown) comes from hydrocarbon reforming (Noussan et al., 2020, p. 2). Reforming is a general term for numerous methods used to convert carbonaceous fuels. At high temperatures, hydrogen (H_2) is created when the hydrocarbon fuel interacts with steam, oxygen (O_2), or a combination of the two (Lamb et al., 2020, p. 29).

There are three hydrocarbon-reforming methods. The reaction is endothermic when only steam is used, and this procedure is known as steam reforming. When oxygen is employed to convert fuel, the reaction is exothermic and is referred to as partial oxidation. The auto-thermal reforming reaction is a combination of the two processes, steam reforming and partial oxidation (Lamb et al., 2020, p. 29)

Natural gas is the most used feedstock for hydrogen production (Speight, 2019, p. 667). With a high hydrogen-to-carbon ratio, this source produces less carbon dioxide during use. In addition, it is simple to handle, unlike oil and coal, which have a low hydrogen-to-carbon ratio and require a significant amount to be provided from steam (Lamb et al., 2020, p. 29).

2.5.1 Steam Reforming

Steam Reforming is also known as Steam Methane Reforming (SMR). The process consists of removing Sulphur from methane and mixing it with water steam in a catalytic process to produce hydrogen and carbon monoxide, as shown in equation 1. In the next step (equation 2), at the water-gas shift reactor (WGS), steam is added to cool down the produced gasses to around 370°C, where carbon monoxide reacts to produce more hydrogen and carbon dioxide. In the last step, carbon dioxide is removed either by passing through scrubbers or by the hot carbonate process, which is more thermally effective. Any carbon oxide remaining is then removed through a methanation process where they react in equations 3 and 4 with hydrogen to produce methane, leaving the produced hydrogen with a purity higher than 99% (Speight, 2019, pp. 675–676).

Reformer	$C_nH_m + nH_2O \longrightarrow nCO + \left(n + \frac{1}{2}m\right)H_2$	Equation 1
WGS	$CO + H_2O \longrightarrow CO_2 + H_2$	Equation 2
Methanation	$CO + 3H_2 \longrightarrow CH_4 + H_2O$	Equation 3
	$CO_2 + 4H_2 \longrightarrow CH_4 + H_2O$	Equation 4

For steam methane reforming, m=1 and n=4 are applied to equation 1 as follows:

Reformer	$CH_4 + H_2O \longrightarrow CO + 3H_2$	Equation 5
WGS reaction	$CO + H_2O \longrightarrow CO_2 + H_2$	Equation 6

Equation 5 shows the H_2/CO ratio of three hydrogen molecules per one carbon monoxide molecule. The WGS reaction in equation 6 yields one additional molecule of hydrogen per molecule of carbon dioxide. Overall, one molecule of methane yields one molecule of carbon dioxide and four molecules of methane (equation 7).

Overall	$CH_4 + 2H_2O \longrightarrow CO_2 + 4H_2$	Equation 7

Figure 7 represents the steam methane reforming process. A standard SMR requires 63 kJ/mol H2, according to measurements. This is roughly equivalent to 30% to 35% of the total natural gas intake in the process (Lamb et al., 2020, p. 32).

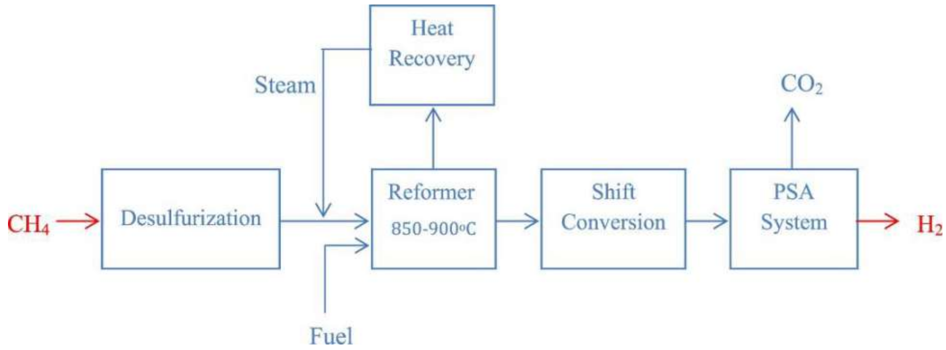

Figure 7. Diagram of SMR process (Nikolaidis & Poullikkas, 2017, p. 600).[2]

Steam reforming can be used with other raw materials to produce hydrogen, such as propane (equation 8) or naphtha (equation 9) which have higher molecular weight as follows (Speight, 2019, pp. 676–680):

$$C_3H_8 + 3H_2O \longrightarrow 3CO + 7H_2 \qquad \text{Equation 8}$$

$$C_6H_{14} + 6H_2O \longrightarrow 6C + 13H_2 \qquad \text{Equation 9}$$

As can be seen, propane and naphtha production yields less hydrogen than methane, which has an H_2/CO ratio of 3/1 (3 molecules of H_2 per 1 molecule of CO), while propane and naphtha yield 2.3/1 and 2.1/1 of H_2, respectively.

SMR is an energy-consuming process due to the endothermic reactions that take place, making it challenging to improve energy efficiency. Thus, the trend in development is towards greater energy efficiency by adapting catalysts and metallurgy to lower steam/carbon ratios and more significant heat fluxes (Speight, 2014, p. 121).

Despite the apparent energy challenge, SMR technology offers the following benefits: (1) it yields four moles of hydrogen per mole of methane; (2) the method can be adapted to a variety of hydrocarbon feedstock; (3) pressure requirements are lower than 450 psi; (4) low steam/carbon ratio, and (5) resistant and stable catalysts (Speight, 2019, p. 679).

[2] Reprinted from Renewable and Sustainable Energy Reviews, Vol 67, Pavlos Nikolaidis, Andreas Poullikkas, A comparative overview of hydrogen production processes, 597-611, Copyright (2017), with permission from Elsevier.

2.5.2 Partial Oxidation (POX)

This process produces carbon oxides and hydrogen by converting oxygen, steam, and hydrocarbons. It is divided into two methods: catalytic (equation 10) and non-catalytic (equation 11). The former takes place at around 950°C using feedstock in the range of methane and naphtha. Without a catalyst, the non-catalytic process takes place at a temperature range of 1150-1325°C converting methane as well as heavy hydrocarbons and coal. As presented in SMR, the water shift reaction (equation 12) and methanation (equation 13) are applied after the POX reaction (Nikolaidis & Poullikkas, 2017, p. 600).

General Eq Catalytic	$C_nH_m + \frac{1}{2}nO_2 \longrightarrow nCO + \frac{1}{2}mH_2$	Equation 10
General Eq Non-Cat.	$C_nH_m + nH_2O \longrightarrow nCO + \left(n + \frac{1}{2}m\right)H_2$	Equation 11
WGS	$CO + H_2O \longrightarrow CO_2 + H_2$	Equation 12
Methanation	$CO + 3H_2 \longrightarrow CH_4 + H_2O$	Equation 13

The preferred technique for producing H_2 from coal and heavy oil is POX. This is because a more significant fraction of the hydrogen produced comes from steam due to the low hydrogen-carbon ratios. POX reactions for heavy oil and coal can be applied in equations 14 and 16, while the WGS is represented by equations 15 and 17 as follows (Nikolaidis & Poullikkas, 2017, p. 600):

Heavy oil, n=1, m=1.3

$$C_{10}H_{13} + 10H_2O \longrightarrow 10CO + 16.5H_2 \qquad \text{Equation 14}$$

$$10CO + 10H_2O \longrightarrow 10CO_2 + 10H_2 \qquad \text{Equation 15}$$

Coal, n=1, m=0

$$C + H_2O \longrightarrow CO + H_2 \qquad \text{Equation 16}$$

$$CO + H_2O \longrightarrow CO_2 + H_2 \qquad \text{Equation 17}$$

Hydrogen production from coal and heavy oil fractions yields less hydrogen than SMR, which has an H_2/CO ratio of 3/1 (equation 5), while heavy oil and coal yield 1.65/1 and 1/1, respectively.

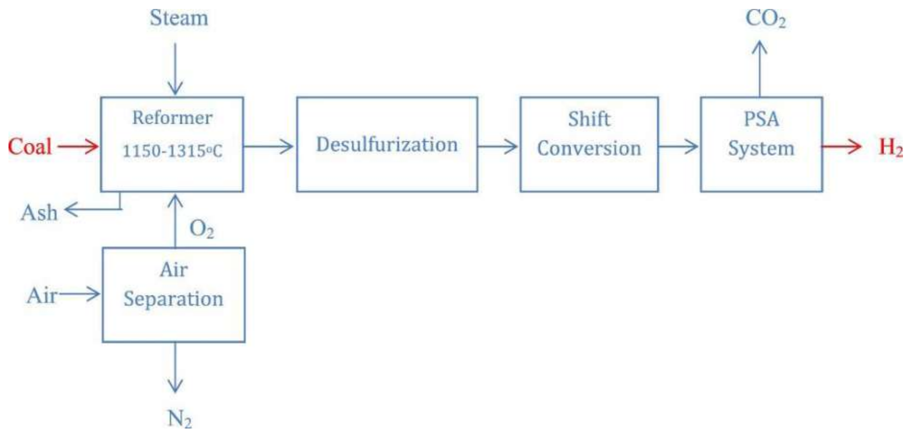

Figure 8. Diagram of Coal Gasification (Nikolaidis & Poullikkas, 2017, p. 601).[3]

The production of hydrogen from coal is also known as coal gasification (Figure 8). This is a necessary process to obtain hydrogen from coal. The chemical reactions in this process closely mimic those in the POX method for heavy oils. However, the low presence of hydrogen in coal means that 83% of the hydrogen produced comes from water steam, while only 69% is supplied from steam when the process uses heavy oil. Moreover, costs are significantly impacted by unburned fuel and ash removal (Nikolaidis & Poullikkas, 2017, p. 600).

2.5.3 Auto Thermal Reforming (ATR)

In the auto-thermal reforming process, oxygen, steam, and hydrocarbon feedstock are mixed in the reformer (Speight, 2014, p. 121). It combines oxidation (POX) and reforming (SR) reactions that take place at the same time, providing heat and increasing hydrogen production, respectively. The general process is described in equation 18 and WGS in equation 19 (Nikolaidis & Poullikkas, 2017, p. 600).

General eq	$C_nH_m + \frac{1}{2}nH_2O + \frac{1}{4}nO_2 \longrightarrow nCO + \left(\frac{1}{2}n + \frac{1}{2}m\right)H_2$	Equation 18
WGS	$CO + H_2O \longrightarrow CO_2 + H_2$	Equation 19

All reactions occur in the reactor, which is divided into three areas. After injection, oxygen, steam, and feedstock are combined in the burner through a turbulent diffusion blaze. Then, partial oxidation takes place in the combustion zone. Finally, the resulting gas mixture reaches the catalyst zone, where the reforming reactions occur via a catalyst bed. In an ideal situation, the auto-thermal reforming process

[3] Reprinted from Renewable and Sustainable Energy Reviews, Vol 67, Pavlos Nikolaidis, Andreas Poullikkas, A comparative overview of hydrogen production processes, 597-611, Copyright (2017), with permission from Elsevier.

might show heat balance since the heat produced in the combustion zone by partial oxidation reactions is used in the reforming zone (Speight, 2014, pp. 121–122).

Using methane (CH_4) as a feedstock in equation 20, where n=1 and m=4, the hydrogen production is lower compared to SMR as the H_2/CO ratio is 2.5/1 (2.5 molecules of H_2 per one molecule of CO). The WGS reaction is presented in equation 21. The ATR for methane is represented in Figure 9 (Nikolaidis & Poullikkas, 2017, p. 601).

$$CH_4 + \frac{1}{2}H_2O + \frac{1}{4}O_2 \longrightarrow CO + \frac{5}{2}H_2 \qquad \text{Equation 20}$$

$$CO + H_2O \longrightarrow CO_2 + H_2 \qquad \text{Equation 21}$$

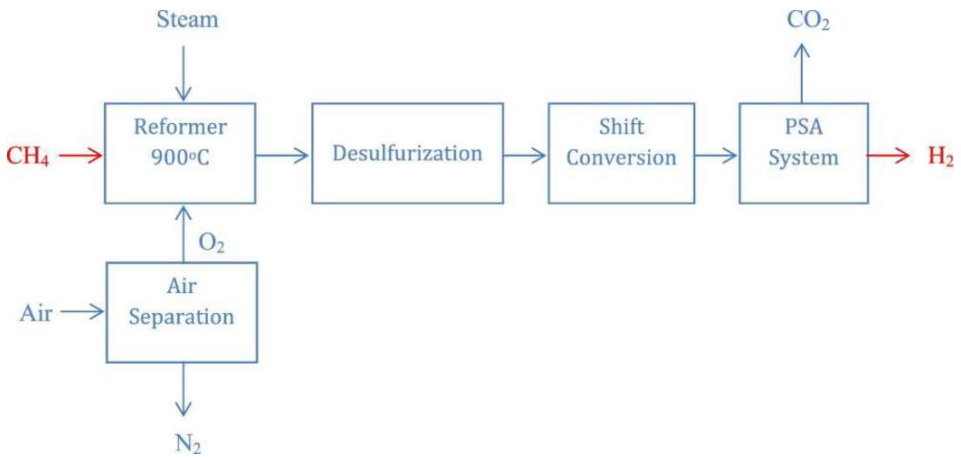

Figure 9. Diagram of ATR of methane (Nikolaidis & Poullikkas, 2017, p. 601).[4]

Utilizing the ATR technique has the following benefits: the minimal need for investment; a compact design resulting in a smaller environmental imprint; economies of scale; a soot-free process, and flexible operation due to quick load changes and short startup time (Speight, 2014, p. 122).

2.6. Carbon Capture Utilization and Storage (CCUS)

This process refers to capturing CO_2 from an emission source or directly from the air and subsequent transportation to reuse or store it permanently (Chen et al., 2022). The use of CO_2 is essential not just for the oil and gas industry, which uses CO_2 in Enhanced Oil Recovery (EOR) applications and provides essential revenue for CCUS projects, but other possible applications of CO_2 in the sector of synthetic

[4] Reprinted from Renewable and Sustainable Energy Reviews, Vol 67, Pavlos Nikolaidis, Andreas Poullikkas, A comparative overview of hydrogen production processes, 597-611, Copyright (2017), with permission from Elsevier.

fuels, chemicals, and construction (IEA, 2020). Figure 10 (IEA, 2020, p. 20) represents the CCUS process of capture, transport, use, and storage.

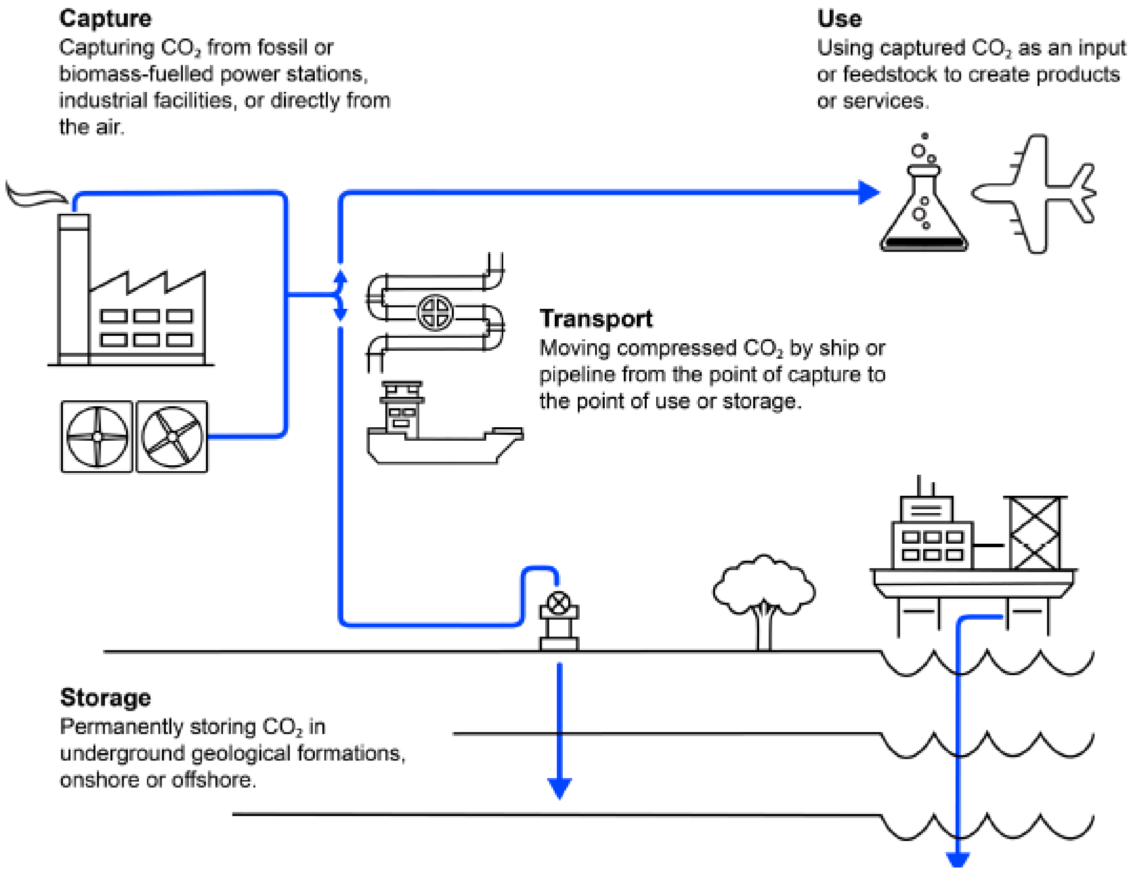

Figure 10. Schematic of CCS (IEA, 2020, p. 20).

Production of hydrogen from fossil fuels releases carbon dioxide (CO_2) into the environment. Thus, using Carbon Capture Utilization and Storage (CCUS) technology can be considered as a link to mitigate CO_2 emissions during the process and to continue allowing the use of fossil fuels as a bridge technology until the implementation of low carbon emission alternatives is in place (Bandilla, 2020, p. 669).

As mentioned, the process consists of three main parts; capture of CO_2 in situ (where the source is), transport, and permanent underground storage. Capture, the first step in this process, refers to capturing CO_2 before or after fossil fuel combustion. For example, in hydrogen production, pre-combustion occurs when the fossil fuel (natural gas) is divided into CO_2 and a fuel (H_2). Then, in favorable operating conditions of high CO_2 concentration and pressure, amino-based solvents remove CO_2. However, one disadvantage is that power plants must be designed to operate with CCS, as retrofitting existing plants is not possible. Figure 11 shows an SMR plant scheme with CCS (Bandilla, 2020, p. 676).

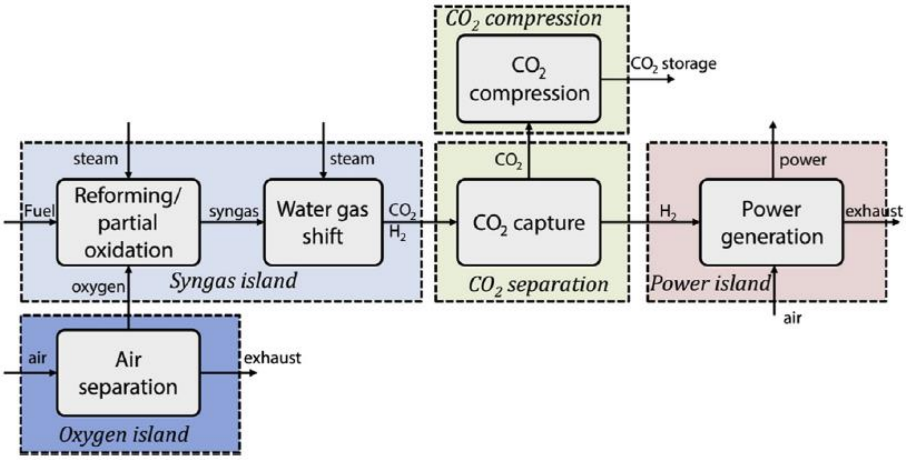

Figure 11. SMR/Partial Oxidation processes scheme with CCS (Bandilla, 2020, p. 676).[5]

After capturing CO_2, transport is required when storage or on-site use is unavailable. In most cases, large amounts of CO_2 must travel long distances to be injected underground for storage or use in enhanced oil recovery (EOR). It is transported in a supercritical state (gas viscosity and liquid density) by pipelines, ships, and trucks. Which means of transport is applicable depends on specific conditions such as CO_2 volume and distance to travel. Supercritical CO_2 density (500 to 750 kg/m^3) reduces the volume required for transportation, and supercritical viscosity decreases the energy that is lost during transmission (Bandilla, 2020, pp. 677–678).

It is expected that pipelines will be the principal method of CO_2 transport due to their large capacity and uninterrupted distribution for CCS applications. Short pipeline connections are used when the capture and storage are at the same site (or relatively close to it) and longer when they are used for EOR applications. Examples of on-site storage are the Illinois Industrial CCS project and the Sleipner Project, while the Snøhvit Project and the Quest Project transport CO_2 through a 170 and 50 km pipeline, respectively (Bandilla, 2020, pp. 678–679).

The construction and operation of pipelines are well-developed. Several pipelines have been built to transport CO_2 for injection in EOR projects. Therefore, in terms of risks, pretreatment of CO_2 to remove moisture is required to avoid corrosion since leaks can cause a loss of pressure and expansion of CO_2, leading to the fracturing

[5] Reprinted from Future Energy, Vol 67, Karl W. Bandilla, 31 Carbon Capture and Storage, 669-692, Copyright (2020), with permission from Elsevier.

of the pipeline. Other events that may cause pipeline failure are manufacturing defects, interference by third parties (accidents), human error, and earthquakes (Bandilla, 2020, pp. 679–680).

The last stage and primary purpose of the CCS process is the storage of CO_2 for an undefined time or at least for extended periods (hundreds of years). In order to store large volumes of CO_2, several options, such as depleted oil and gas reservoirs and saline formations, have been successfully tested. At the same time, unmineable coal seams were not successful in their pilot stage. However, deep ocean storage is a strategy that has yet to be tested due to safety and environmental concerns such as ocean acidification and detriment to local marine life (Bandilla, 2020, p. 681).

In depleted oil and gas reservoirs, CO_2 is stored in a porous sedimentary rock (siliclastic or carbonate). The pores of these rocks are usually filled with oil, gas, and water (or a mix) to determine how much volume of a fluid the rock can store. The percentage between the pore space divided by the total rock volume is called 'porosity'. The higher the porosity, the more fluid it can store. Another important property is 'permeability', which refers to the ease with which fluids can move through porous rock and depends on the size and connection of the pores. Storage in saline aquifers is similar to that in-depleted oil and gas reservoirs, with the difference that the pores are occupied with saltwater (Bandilla, 2020, p. 681).

Injection of CO_2 is done via drilled wells that connect the surface to the reservoir located 800 meters or more profoundly. At this depth, temperature and pressure keep CO_2 in supercritical condition to allow its migration through the pores due to low viscosity and smaller volume. Migration of CO_2 continues until it finds a seal rock, which is impermeable, stopping migration and trapping the CO_2 underground. Capillary trapping is a secondary process where CO_2 is caught in the pores due to capillarity while it migrates through the reservoir. Dissolution is the third and less effective process, where a small volume of CO_2 (less than 5%) dissolves into the water. The density of this mix is denser than water. Thus, it will go downward rather than upward, stopping CO_2 migration (Bandilla, 2020, pp. 681–682).

The success of the CCUS process lies in storing the CO_2 in the subsoil. Therefore, storage safety is essential when talking about CO_2 leaks from the reservoir. Furthermore, natural faults and fractures of the seal rock are the main issues followed by active or abandoned wells made by the oil and gas industry. Therefore, particular parameters are in place to control the maximum percentage of allowed CO_2 leaks from the reservoir (Bandilla, 2020, p. 682).

2.7. Water Electrolysis

Electrolysis is the process in which water is broken up into hydrogen and oxygen (see equation 22) by applying an electrical current (IEA, 2021a). This electrochemical route yields pure H_2 and is considered a zero-emissions technology when using renewable electricity (e.g. wind, and solar) (Shiva Kumar & Himabindu, 2019).

$$H_2O \longrightarrow H_2 + \frac{1}{2}\,O_2 \qquad \text{Equation 22}$$

In broad terms, it consists of applying direct current to an anode and a cathode immersed in a conductive electrolyte. In the anode, oxidation takes place to produce oxygen, whereas, in the cathode, reduction occurs for hydrogen production (Braga et al., 2017a, p. 34).

2.8. Electrolyzers

The whole process occurs in an electrochemical device called an ‘electrolyzer’. There are four leading technologies for H_2 production through water electrolysis. As of 2020, Alkaline (AEL) and proton exchange membrane (PEM) lead the market with 61% and 31% share of the total installed capacity. Conversely, solid oxide electrolysis cells (SOECs) have less than 1%, and the remaining percentage is held by solid anion exchange membranes (AEMs) and unknown technologies, as shown in Figure 12 (IEA, 2021a).

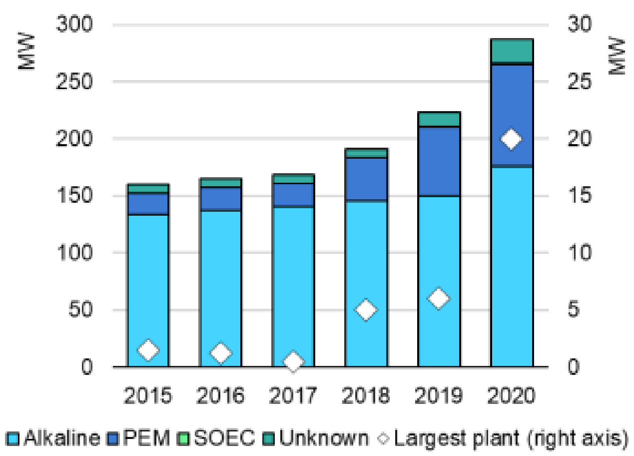

Figure 12. Global installed capacity by technology (IEA, 2021a, p. 116).

2.8.1 Alkaline Electrolysis (AEL)

Alkaline electrolysis is an established mature technology with 62-82% efficiency that can yield between 1 to 760 Nm^3H_2/h, with electrodes and membranes requiring maintenance every eight years and up to 30 years total. Basically, two electrodes are immersed in a liquid solution of either NaOH or KOH with a concentration between 25-30% in which reactions take place to produce O_2 from the anode and H_2 from the cathode in equation 23 as follows (Braga et al., 2017a, p. 36):

$$\text{Anode:} \qquad 4OH^- \longrightarrow O_2 + 2H_2O + 4e^-$$

$$\text{Cathode:} \qquad 4OH^+ + 4e^- \longrightarrow 2H_2$$

$$\text{Total:} \qquad 2H_2O \longrightarrow O_2 + 2H_2 \qquad \text{Equation 23}$$

A permeable membrane is placed between the two electrodes to allow OH^- ions to pass through while gases are retained. Common materials are used to manufacture the electrodes, such as steel and carbon, whereas nickel is used to cover the anode to avoid corrosion. They are up to 5 mm apart from each other, with a maximum operating temperature of 80°C (Braga et al., 2017a, p. 37). The working scheme is specified in Figure 13 (IRENA, 2020b, p. 31).

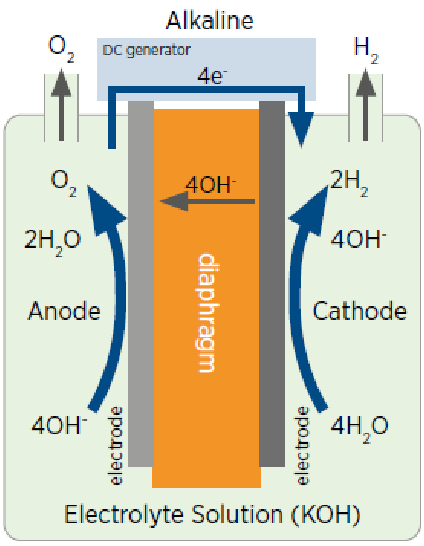

Figure 13. Alkaline electrolyzer scheme. Adapted from IRENA (2020b, p. 31).

Alkaline electrolyzers can be operated at low pressures of up to 6 bar and high pressures between 6 and 30 bar. When operating at high pressure, produced hydrogen is already compressed. However, the purity of the hydrogen tends to reduce as permeability in the membrane increases. Therefore, in terms of the electrolyzers' energy demand, 4.1 to 4.5 kWh/Nm^3H_2 is needed in low-pressure conditions (or up to 7 kWh/Nm^3H_2 if H_2 is compressed). On the other hand, 4.5 to 5 kWh/Nm^{3}H$_2$ is required when using high-pressure conditions (Braga et al., 2017a, p. 37).

Although the produced hydrogen may contain unwanted elements such as oxygen and water vapor that require additional purification steps, this technology requires lower initial capital, has well-known operational costs, and large capacity demonstrations have been reached when compared with the other technologies for water electrolysis (Lamb et al., 2020).

2.8.2 Proton Exchange Membrane (PEM)

PEM is also known as Solid Polymer Electrolite (SPE), where the conductive electrolyte NaOH or KOH) is replaced by a thin polymer membrane (less than 0.2 mm) that allows the electrodes to be closer to each other. In this process, the oxidation of water takes place at the anode to produce protons (H+), electrons (e-), and oxygen (O_2). Then, protons move through the membrane and are transformed at the cathode into pure hydrogen (Braga et al., 2017a, p. 38). Equation 24 represents the reactions in the process (Lamb et al., 2020, p. 40).

$$\text{Anode:} \quad H_2O \longrightarrow \frac{1}{2}O_2 + 2H^+ + 2e^-$$

$$\text{Cathode:} \quad 2H^+ + 2e^- \longrightarrow H_2$$

$$\text{Total:} \quad H_2O \longrightarrow H_2 + \frac{1}{2}O_2 \qquad \text{Equation 24}$$

Usually, operation conditions of up to 15 bar and 80°C yield 99.99% pure hydrogen with 67% to 82% efficiency. Production capacity is between 0.06 and 30 Nm^{3}H^2/h, and the energy demand ranges between 4.5 to 7 kWh/Nm^{3}H$_2$. Despite its high investment cost due to expensive materials such as electrodes and membranes and being still in a developmental stage, it is not affected by electricity fluctuation as it occurs with variable renewable energy sources. This makes it possible to use it as energy storage (Braga et al., 2017a, p. 39). Figure 14 represents the PEM electrolyzer scheme (IRENA, 2020b, p. 31).

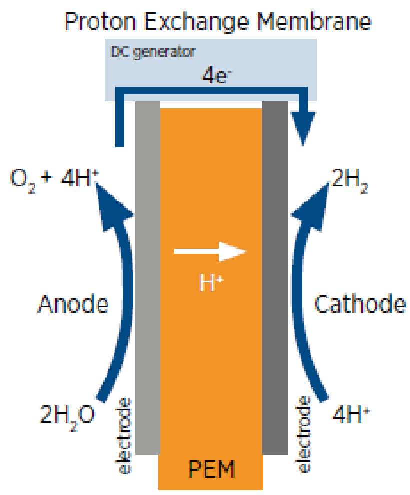

Figure 14. PEM electrolyzer scheme. Adapted from IRENA (2020b, p. 31).

Commercial PEM electrolyzers yield more than 99.99% pure hydrogen, having oxygen as the most significant unwanted element. They are characterized by the low energy demand of 3.9 kWh/Nm^{3}H$_2$ at 1 A/cm^2 (current density), more than 10,000 hours of operation lifespan, and delivery of high-pressure Hydrogen. Currently, state-of-the-art in the market uses iridium oxide and platinum in the anode and cathode, respectively. This configuration has 80% of enthalpy efficiency and a current density between 1.0 to 1.5 A/cm^2 (Lamb et al., 2020, p. 42).

2.8.3 Solid Oxide Electrolyte Electrolysis (SOEL)

High-Temperature Electrolysis (HTEL) or SOEL performs the electrolytic process using temperatures between 600 and 1000ºC. By applying this technology, water in the form of steam is reduced at the cathode at high temperatures to produce hydrogen and oxide anions, which later move to the anode through the solid electrolyte to be recombined and produce oxygen (Braga et al., 2017a, pp. 39–40). Equation 25 represents the electrochemical process mentioned above (Lamb et al., 2020, p. 43):

$$\text{Anode:} \qquad O^{2-} \longrightarrow \frac{1}{2}O_2 + 2e^-$$

$$\text{Cathode:} \qquad H_2O + 2e^- \longrightarrow H_2 + O^{2-}$$

$$\text{Total:} \qquad H_2O \longrightarrow H_2 + \frac{1}{2}O_2 \qquad \text{Equation 25}$$

The solid electrolyte, placed in the middle of the electrodes, is made of yttrium and zirconia (YSZ). The anode consists of perovskite ($CaTiO_3$), and the cathode is a metal alloy with nickel particles and YSZ (Braga et al., 2017a, p. 40). The SOEL process can be seen in Figure 15 (IRENA, 2020b, p. 31).

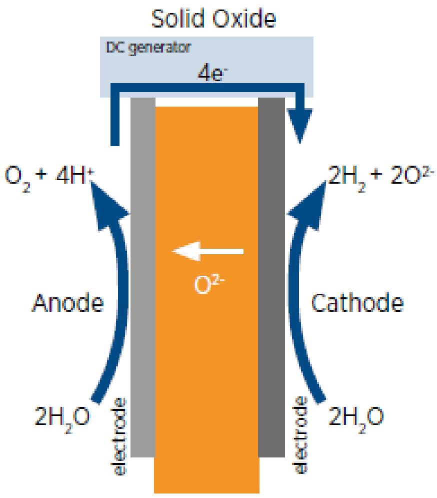

Figure 15. SOEL process scheme. Adapted from IRENA (2020b, p. 31).

Demand for SOEL has increased due to the potential of operating it at high efficiencies and high-current densities (3.6 A/cm^2), making it a good option for reducing CO_2 emissions in the energy sector. Another advantage is that the electrochemical process is reversible as it operates at high temperatures. Additionally, syngas (H_2 + CO) production may be possible when using water in the form of steam and carbon dioxide (CO_2) in a process called co-electrolysis. Then, the syngas can produce synthetic fuels (Lamb et al., 2020, pp. 43–44).

2.8.4 Anion Exchange Membrane Electrolysis (AEMEL)

AEMEL technology is still in the research and development stage. Its potential stands out due to the low cost of materials and its high stability. However, more research is required to overcome current disadvantages regarding the process's general performance (Vincent & Bessarabov, 2018).

The electrochemical process involves splitting water into H_2 by applying a direct external current. Reduction of water into H_2 and OH^- ions occurs at the cathode. The OH^- ions move to the anode through the anion exchange membrane (AEM) to form O_2 and H_2O. Pure water (distilled) or an alkaline solution in low concentration is used as an electrolyte. Equation 26 represents the electrochemical reactions (Vincent & Bessarabov, 2018, p. 1693):

$$\text{Anode:} \qquad 4OH^- \longrightarrow O_2 + 2H_2O + 4e^-$$

$$\text{Cathode:} \qquad 4H_2O + 4e^- \longrightarrow 2H_2 + 4OH^-$$

$$\text{Total:} \qquad 2H_2O \longrightarrow 2H_2 + O_2 \qquad \text{Equation 26}$$

The membrane (AEM) is a carrier for OH^- ions and a barrier for electrons and gases produced in the process. The electrodes are made of non-noble metals, decreasing the cost of the process. This non-noble metal can be an alloy like Ni-Fe, nickel (Ni), or iridium oxide (IrO2), among others, which are used in the anode. For the cathode, platinum (Pt) black, CuCoOx, and Ni-Mo, among others, are used (Vincent & Bessarabov, 2018). Figure 16 represents the AEM technology (IRENA, 2020b, p. 31).

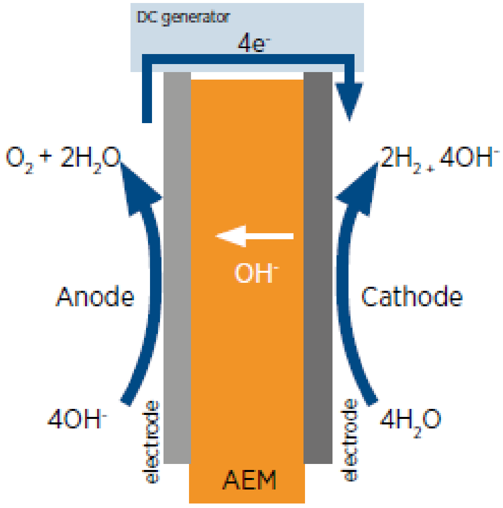

Figure 16. AEM process scheme. Adapted from IRENA (2020b, p. 31).

As the AEM technology is still in its early stages, the capital costs of the system will be reduced by using transitional metals as electrodes (Vincent & Bessarabov, 2018). However, system durability and performance must be addressed by improving membrane stability (chemical and mechanical) and reaching higher conductivity, better electrode architectures, and faster catalyst kinetics (IRENA, 2020b).

2.9. Technologies Comparison

Table 4 summarizes the advantages and disadvantages of the different methods of producing low-carbon hydrogen.

Table 4. Comparison of the different hydrogen production processes. Adapted from Nikolaidis & Poullikkas (2017, p. 608).[6]

Process	Efficiency (%)	Major advantages	Major disadvantages
SR	74-85	Most advanced technology, existing infrastructure.	CO_2 byproduct, dependence on fossil fuels.
POX	60-75	Proven technology and existing infrastructure.	CO_2 byproduct, dependence on fossil fuels.
ATR	60-75	Proven technology and existing infrastructure.	CO_2 byproduct, dependence on fossil fuels.
Electrolysis	40-60	No pollution with renewable sources, proven technology, existing infrastructure, abundant feedstock, O_2 is the only byproduct, contributes to RES integration as an electricity storage option.	Low overall efficiency, high capital costs.

[6] Reprinted from Renewable and Sustainable Energy Reviews, Vol 67, Pavlos Nikolaidis, Andreas Poullikkas, A comparative overview of hydrogen production processes, 597-611, Copyright (2017), with permission from Elsevier.

3 Methodological Approach

This thesis aims to determine whether blue hydrogen (coal, oil, and gas) production is needed in the short term to achieve green hydrogen production (electrolysis using electricity by wind and solar PV) in the long term and reduce the current trend in CO_2 emissions. Other low-carbon technologies, such as methane pyrolysis, biomass, hydro, and nuclear power, among others, are not considered due to the limited scope of this thesis.

The world is calling to keep temperatures below two degrees Celsius by 2050 to avoid serious consequences (IPCC, 2022). To achieve this, blue hydrogen could help hydrogen deployment to move towards clean technologies for energy production worldwide. For that reason, low carbon (green and blue) hydrogen production (IEA, 2021a) and its deployment is the main topic for institutions, research, and governments today. To assess $CO_{2\text{-eq}}$ emissions in this thesis, there will be two analytical timeframes: short-term refers to hydrogen demand and its emissions in 2030, while long-term refers to hydrogen demand and its emission in 2050.

Within the scope of this thesis, the following research questions will be addressed:

What are the benefits of producing blue H_2 in the short-term to achieve total green H_2 production in the long-term regarding CO_2 emissions?

- What is the expected gray, blue, and green hydrogen share in 2030 and 2050?
- What are the CO_2 emissions when producing gray, blue, and green hydrogen?
- Will blue H_2 production reduce CO_2 emissions in the short and long-term?

The research method will consist of a qualitative literature review using peer-reviewed articles and gray literature such as national hydrogen strategies, industry reports, websites, and news articles. The first step is to conduct an industry overview of the two technologies, the status quo, and their prospects through market research of blue and green hydrogen and analyzing the findings according to technological status and emissions.

Secondly, the carbon intensity in kg $CO_{2\text{-eq}}/kgH_2$ for gray, blue, and green hydrogen will be taken from the literature review to calculate the $CO2_{\text{-eq}}$ (CO_2 and CH_4) emissions from the expected hydrogen demand in 2030 and 2050. There will be scenarios with low and high carbon capture (CCS) to analyze the impact of blue hydrogen technology. The share of every color (gray, blue, and green) of hydrogen in million tons (Mt) will determine the total $CO_{2\text{-eq}}$ emissions in every proposed scenario. The global warming potential (GWP) plays a vital role in the literature as there is no consensus among authors about which of the two is the most appropriate. GWP20 measures the impact of $CO_{2\text{-eq}}$ emissions in 20 years, whereas GWP100 does so in 100 years. Therefore, this thesis will use carbon intensities calculated with a GWP20 and GWP100 from the literature for calculation and future comparison.

This thesis will compare $CO2_{\text{-eq}}$ emissions from gray, blue, and green hydrogen production in the short and long term. Therefore, the economic analysis is not considered.

For this thesis, the selection of included peer-reviewed articles and articles was made by a keyword search on sciencedirect.com and researchgate.net. The following keywords were used: green hydrogen, blue hydrogen, hydrogen production, hydrogen demand, hydrogen strategy, hydrogen emissions, CCUS, and CCS. By screening the articles and filtering those which did not match the topic and scope of this thesis, the final number of papers was reduced to 10.

4 Literature Review

There is a clear path to developing hydrogen to decarbonize industrial and domestic sectors to reduce CO_2 emissions. In this chapter, available literature describes the status of blue and green hydrogen and the climate impact from different authors' perspectives. Future hydrogen demand has also been estimated according to the future needs in industry, transport, buildings, and electricity generation, among others, by institutions and researchers who have different ideas about how hydrogen will be utilized in the future. Countries will supply this demand through their national hydrogen strategies to promote and support the development and deployment of blue and green hydrogen.

4.1. Green Hydrogen Status

Green hydrogen production via water electrolysis was represented by around 320 demonstration projects in 2020, which corresponded to less than 0.02% of total hydrogen production. Most of these projects have a capacity of less than 10 MW (IRENA, 2020b, p. 18). However, the most significant demonstration projects in 2022, as shown in Table 5, are two of 10 MW in Germany and Japan and one of 20 MW in Canada (IEA, 2022a).

Table 5. Green hydrogen's most significant demonstration projects. Own table based on IEA (2022a), REFHYNE (2022), Patel (2022), Suda (2021), Air Liquide (2021).

Country	Facility	Capacity (MW)	H_2 production capacity (ton/yr)	H_2 Production Technology	H_2 Use	Timing
Germany	Refhyne	10	1,300	PEM	Petroleum refining	2021
Japan	FH2R	10	900	AEL	Fuel cell batteries	2020
Canada	Air Liquide Becancour	20	3,000	PEM	Industrial use and mobility	2020

Alkaline and PEM electrolyzers are leading the electrolyzers market in terms of capacity and technology development, whereas AEM and SOEC electrolyzers are still in the R&D stage. However, they all produce high-purity hydrogen (IRENA, 2020b), as seen in Table 6.

Table 6. State-of-the-art for all electrolyzer technologies. Adapted from IRENA (2020b, pp. 65-66).

	Alkaline	PEM	AEM	SOEC
Technology status	Commercial	Commercial	Lab scale	Lab scale
Nominal current density (A/cm2)	0.2-0.8	1-2	0.2-2	0.3-1
Voltage range (V)	1.4-3	1.4-2.5	1.4-2.0	1.0-1.5
Operating temperature (ºC)	70-90	50-80	40-60	700-850
Cell pressure (bar)	30	< 30	< 35	1
Load range (%)	15-100	5-120	5-100	30-125
H_2 Purity (%)	99.9-99.9998	99.9-99.9999	99.9-99.999	99.9
Voltage efficiency (LHV) (%)	50-68	50-68	52-67	75-85
Efficiency (system) (kWh/kgH_2)	50-78	50-83	57-69	40-50
Lifetime (thousand hours)	60	50-80	> 5	< 20
Stack unit size (MW)	1	1	0.0025	0.005
Cold start (to nominal load) (min)	< 50	< 20	<20	> 600

The technology for producing alkaline water hydrogen is mature, the manufacturing costs are low, and a total of 1000 m^3/h of hydrogen has been reached. However, this technology has drawbacks such as slow startup, corrosion, complicated maintenance, and many device components. The advantages of PEM hydrogen production technology include faster start-up, no corrosion, and simple maintenance. The technology has reached a production of 400 m^3/h of hydrogen. However, the main factors limiting the development of PEM technology are high manufacturing costs (Guo et al., 2019, p. 5). These high manufacturing costs refer to critical materials used in both Alkaline and PEM electrolyzers. To allow large-scale deployment, alkaline electrolyzers must avoid nickel and platinum in their designs. In contrast, PEM electrolyzers need to reduce the use of platinum and iridium, which are rare, and energy and carbon-intensive materials. AEM electrolyzers do not use scarce and expensive materials such as platinum and iridium, having an advantage over PEM. Thus, there is a significant cost reduction potential compared to PEM electrolyzers. It also operates under differential pressure. However, its membrane possesses stability problems (chemical and mechanical), showing a shorter lifetime and low performance due to durability and conductivity. SOEC electrolyzers can use nickel electrodes, which is considered a cheap material, as it operates at high temperatures. The promise of solid oxide is substantially improved efficiency, which translates into more affordable electricity prices. However, SOEC electrolyzers have faster degradation and a shorter lifetime due to thermo-chemical cycling during startup and shutdown (IRENA, 2020b).

The expected development of the four technologies is presented in Table 7 (IRENA, 2020b, pp. 65–66). By 2050, IRENA (2020b) set a future trend and defined which properties of every electrolyzer could be improved. Despite the stage of development in Table 6, current density, cell pressure, and lifetime are expected to increase, allowing for more H_2 production and better compression and durability of the systems (IRENA, 2020b).

Table 7. Future KPIs for all electrolyzer technologies. Adapted from IRENA (2020b, pp. 65–66).

	2050			
	Alkaline	PEM	AEM	SOEC
Nominal current density (A/cm2)	> 2	4-6	> 2	> 2
Voltage range (V)	1.7	< 1.7	< 2	< 1.48
Operating temperature (ºC)	> 90	80	80	< 600
Cell pressure (bar)	>70	> 70	> 70	> 20
Load range (%)	5-300	5-300	5-200	0-200
H_2 Purity (%)	> 99.9999	99.9-99.9999	> 99.999	> 99.9999
Voltage efficiency (LHV) (%)	> 70	>80	> 75	> 85
Efficiency (system) (kWh/kgH_2)	< 45	< 45	< 45	< 40
Lifetime (thousand hours)	100	100-120	100	80
Stack unit size (MW)	10	10	2	0.2
Cold start (to nominal load) (min)	< 30	< 5	< 5	< 300

It is expected to move the electrolysis technologies to the GW scale and bring them to reality. To achieve this, the aims are to reduce cost, improve durability, and increase efficiency. This will necessitate economies of scale, increased production capacity, and technical advances via research (IRENA, 2020b). Table 8 (IRENA, 2020b, pp. 59–63) shows the challenges that need to be addressed in R&D for every technology to obtain high benefits.

Table 8. Proposed activities to improve the performance of all electrolyzers. Adapted from IRENA (2020b, pp. 59–63).

Technology	Activities to improve performance	Challenge
Alkaline	Improved kinetics for both hydrogen and oxygen evolution with novel nickel-based alloys.	Moderate
	Mitigate critical degradation of catalysts on the anode side to avoid loss of surface area.	Difficult
	Eliminate mechanical degradation of catalyst layers (delamination, dissolution).	Difficult
	Identify stable polymer chemistry that can be used as an ionomer (OH- transport) to fabricate electrodes for alkaline electrolyzers.	Difficult
	Identify stable polymer chemistry that can be used as an ionomer (OH- transport) to fabricate electrodes for alkaline electrolyzers.	Difficult
PEM	Increase catalyst utilization of anode and cathode catalysts.	Moderate
	Reduce the ohmic losses and gas permeation of PFSA membranes.	Difficult
	Improve kinetics for oxygen evolution using iridium-free catalysts and maintain stability comparable to iridium SoA.	Difficult
	Create noble metal-free protective layers for PTLs.	Difficult
	Create titanium-free PTLs.	Difficult
AEM	Reducing the ohmic losses and gas permeation of AEM membranes.	Moderate
	Improve kinetics for hydrogen and oxygen evolution and maintain long-term stability.	Moderate
	Increase AEM membrane durability.	Difficult
	Eliminate mechanical degradation of catalyst layers (delamination, dissolution) and improve ionomer/catalyst binding properties.	Difficult
SOEC	Solve challenges related to lanthanum manganite (LSM) or lanthanum ferrite (LSF) delamination from the electrolyte.	Moderate
	Improve kinetics for hydrogen and oxygen evolution and maintain long-term stability.	Difficult
	Eliminate thermal instability issues caused by an expansion coefficient mismatch between electrolytes and electrodes.	Difficult
	Scaling up of stack components towards larger stack MW units.	Difficult

In terms of CO_2 emissions, Valente et al. (2017) performed an LCA harmonization through a defined protocol of renewable hydrogen production from 71 different studies. The standard conditions for hydrogen are the same in all studies and are the following: final pressure of 20 MPa, compression at 25^{0}C, 75% efficiency, and a purity of 99% or higher (Valente et al., 2017, p. 764). The hydrogen production methods that are considered in this study are thermochemical (biomass/biofuel reforming and gasification and thermochemical cycles), electrochemical (water electrolysis), and biological (biomass fermentation). The study harmonized the methodological aspects of each case study. In the first step, the generic modeling technique, the LCIA method, and the system boundaries are discussed, considering the GWP100, IPCC factors for CO_2, N_2O, and CH_4, and hydrogen production/purification as the last stage. Then, a functional unit of 1 kgH_2 is used or converted using LHV, where it is not directly specified. The multi-functionality of the system, where hydrogen is the main product or a by-product, is analyzed to identify the carbon footprint in each subsystem. In the last step, the boundary of the system is defined up to the compression stage, and it is added where needed. The GWP of capital goods linked to every stage of the system is added depending on the type of plant. Harmonization is shown to have a greater impact on the thermochemical and biological production methods than on the electrochemical ones. Of the 71 harmonized studies, 28 correspond to water electrolysis from wind and solar PV, as shown in Table 9 (Valente et al., 2017, pp. 767, 770).

Table 9. Original and harmonized GWP of renewable hydrogen within the electrochemical category (wind and solar PV). Adapted from Valente et al. (2017, pp. 767, 770).[7]

Green H_2 production process	Code	Original GWP* kg CO2-eq / kgH_2	Harmonized GWP kg CO2-eq / kgH_2
Water electrolysis (wind power)	WPE1	3.33	1.08
Water electrolysis (wind power)	WPE2	2.46	0.97
Water electrolysis (wind power)	WPE3	0.97	0.96
Water electrolysis (wind power)	WPE4	0.87	0.96
Water electrolysis (wind power)	WPE5	0.38	0.51
Water electrolysis (wind power)	WPE6	1.85	2.02
Water electrolysis (wind power)	WPE7	0.97	1.15
Alkaline water electrolysis (wind power)	WPE8	1.09	1.20
Alkaline water electrolysis (asbestos membrane) (wind power)	WPE9	0.62	0.73
Alkaline water electrolysis (advanced membrane) (wind power)	WPE10	0.57	0.68
Alkaline water electrolysis (asbestos membrane) (wind power)	WPE11	0.57	0.68
Alkaline water electrolysis (Na-Cl cell) (wind power)	WPE12	0.03	0.16
Alkaline water electrolysis (wind power)	WPE13	0.76	0.85
Alkaline water electrolysis (wind power)	WPE14	0.63	0.78
PEM water electrolysis (wind power)	WPE15	0.60	0.74
High-temperature water electrolysis (Wind power)	WPE16	0.51	0.63
Alkaline water electrolysis (wind power)	WPE17	0.85	0.84
High-temperature electrolysis (intermittent wind power)	WPE18	0.69	0.81
High-temperature electrolysis (intermittent wind power; biogas reforming back-up)	WPE19	2.18	2.29
Alkaline water electrolysis (photovoltaic power)	PVE1	2.18	2.18

[7] Reprinted from Journal of Cleaner Production, Vol 149, Antonio Valente, Diego Iribarren, Javier Dufour, Harmonised life-cycle global warming impact of renewable hydrogen, 762-772, Copyright (2017), with permission from Elsevier.

Water electrolysis (photovoltaic power)	PVE2	2.41	2.59
Water electrolysis (photovoltaic power)	PVE3	8.00	5.75
Water electrolysis (photovoltaic power)	PVE4	3.66	3.98
Water electrolysis (photovoltaic power)	PVE5	2.15	2.37
Alkaline water electrolysis (Na-Cl cell) (photovoltaic power)	PVE6	0.37	0.69
PEM water electrolysis (photovoltaic power)	PVE7	3.0	3.22
Alkaline water electrolysis (photovoltaic power)	PVE8	5.82	5.04
Alkaline water electrolysis (photovoltaic power)	PVE9	6.50	7.54
**Up to the H_2 compression or liquefaction stage (when reported in the original case study; otherwise, up to the stage before compression/liquefaction.)*			

The authors harmonized one SMR as a base case, yielding a GWP of 12.95 $kgCO_{2eq}/kgH_2$ (Valente et al., 2017, p. 768). Compared to renewable hydrogen via water electrolysis from wind and solar PV, renewable hydrogen outperforms conventional SMR in terms of GWP. The authors also stated that the results indicate that using wind power as the driving energy is generally a convenient alternative for low-carbon hydrogen. Hydropower and other power sources, on the other hand, are shown to be conditioned by power plant size (Valente et al., 2017).

Bauer et al. (2022) compared the climate impact of blue and green hydrogen from water electrolysis. The authors estimated that utilizing solar PV electricity for electrolysis in northern latitudes represents the top of the spectrum of $CO_{2\text{-}eq}$ emissions from green hydrogen while using hydropower represents the lower emissions. Thus, emissions are nearly zero to around 3 $kgCO_{2eq}/kgH_2$. On the other hand, emissions from performing electrolysis with average electricity from the grid in either the US or Europe are significantly higher than those from renewable electricity (Figure 17) (Bauer et al., 2022).

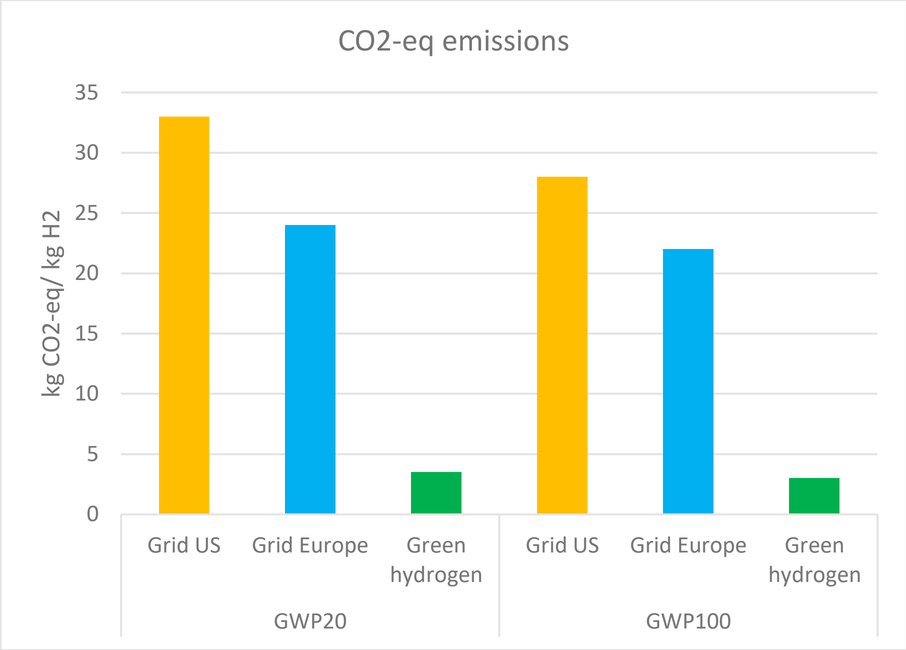

Figure 17. Impacts on climate change associated with green hydrogen and electrolysis from average grid electricity in Europe and the US. Adapted from Bauer et al. (2022, p. 70).

This value does not include the climate impact of using batteries to deal with the intermittency when the electricity is 100% from renewable sources (wind and solar PV) and electricity from the grid is not supplied (Bauer et al., 2022). This increase has been quantified to be in the order of 10% for a given system configuration (Palmer et al., 2021).

4.2. Blue Hydrogen Status

In 2021, according to the Global CCS institute, there were seven blue hydrogen production facilities at a commercial scale operating in the world, as shown in Table 10 (Global CCS Institute, 2021, p. 56). From this data, more than 50% of plants with CCS run with natural gas as a feedstock through SMR, whereas coal gasification has a share of 14%. Of the seven commercial facilities, the Quest Plant in Canada is the only one that captures and storages the CO_2 in a saline aquifer 2 km under the surface (Rock et al., 2017, p. 5322). The remaining plants capture and transport the CO_2 to be used in enhanced oil recovery (EOR) applications (Longden et al., 2022, p. 4).

Table 10. Hydrogen production capacity with CCS (Global CCS Institute, 2021, p. 56).

Facility	H_2 production capacity (ton/day)	H_2 production process	H_2 use	Operational Commencement
Enid Fertilizer	200 (in syngas)	Methane reformation	Fertilizer production	1982
Great Plains Synfuel	1300 (in syngas)	Coal gasification	Synthetic natural gas production	2000
Air Products	500	Methane reformation	Petroleum refining	2013
Coffeyville	200	Petroleum coke gasification	Fertilizer production	2013
Quest	900	Methane reformation	Bitumen upgrading (synthetic oil production)	2015
ACTL Sturgeon	240	Asphaltene residue gasification	Bitumen upgrading (synthetic oil production)	2020
ACTL Nutrien	800	Methane reformation	Fertilizer production	2020

Moreover, 18 new projects where blue hydrogen is produced as an intermediate or final product are in development. Most of the projects (13 out of 18) are located in Europe, followed by the US with two and New Zealand, Indonesia, and Canada with one each. They are expected to start operation between 2022 and 2030 (Global CCS Institute, 2021, p. 58).

The literature available provides insight into blue hydrogen production and its climate impact along the whole supply chain, from natural gas exploration and production to hydrogen transport and storage. Analysis and comparisons between blue hydrogen production methods and conventional use of fossil fuels for heating are given with different modeling and assumptions. Researchers are divided on the topic of how blue hydrogen can be further developed in the upcoming years to accomplish the goal of reducing CO_2 emissions.

Howarth & Jacobson (2021) calculated systematic CO_2 emissions from gray hydrogen and blue hydrogen via SMR, whereas hydrogen from coal gets the color 'brown' and is not considered for this study. The authors considered methane emissions associated with natural gas exploration, production, processing, and transport. Moreover, the Global Warming potential of 20 years (GWP20) is preferred as natural gas remains in the atmosphere for around 12 years and has a warming effect of 86-times as CO_2 when comparing both gases at the same time (Howarth & Jacobson, 2021, pp. 4–5). They explain that CO_2 is produced directly from two sources in the SMR process, the flue gas after natural gas is burned to drive the

SMR (required heat and high pressure) and the CO_2 when reforming methane into hydrogen. The authors also mentioned that when adding the carbon capture, a calculation to capture emissions from these two sources is made, noting that as of 2021, only CO_2 is captured from the SMR process in two commercial facilities, leaving aside the emissions generated by burning natural gas to run the process. Thus, for their study, CO_2 emissions from the flue gas stream and from the required electricity to power the carbon capture were calculated (Howarth & Jacobson, 2021, pp. 2–5). Based on their calculation, overall capture efficiencies and estimates are assumed in this thesis to be 47% when only flue gas is captured and 76% when CO_2 from both sources is captured (Own calculation based on Howarth & Jacobson (2021, p. 5)).

Furthermore, indirect CO_2 emissions associated with producing and transporting natural gas are also included. The authors used the HHV and assumed a methane leakage rate of 3.5% (an average estimate from natural gas fields in the US). The calculated CO_2 and CH_4 emissions in $CO_{2\text{-eq}}$ are presented in Figure 18 (Howarth & Jacobson, 2021, p. 8).

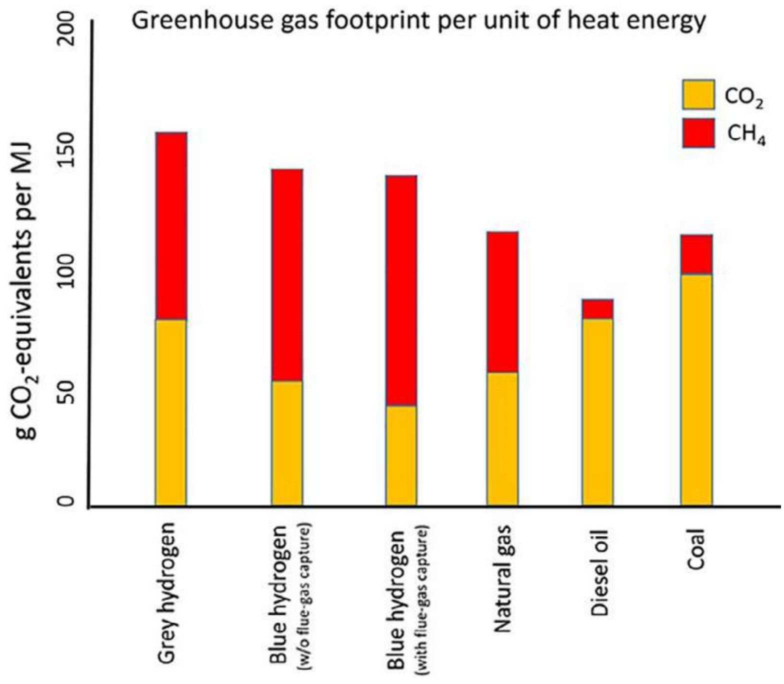

Figure 18. Comparison of carbon dioxide equivalent emissions for different fuels (Howarth & Jacobson, 2021, p. 8).

According to this study (Figure 18), burning natural gas, diesel oil, and coal for heating purposes produce less CO_2 per unit of energy (MJ) than converting natural gas into hydrogen with or without CCS. However, the reduction of CO_2 emissions from blue hydrogen (9-12%) is insignificant compared to those from gray hydrogen

(Howarth & Jacobson, 2021, p. 1). Therefore, although the emissions for transporting and storing the CO_2 are not considered and assuming the captured CO_2 is stored indefinitely, the authors believed that blue hydrogen is not 'low emissions' and concluded that there is no benefit to using blue hydrogen fueled by natural gas as opposed to just using the gas itself for heating (Howarth & Jacobson, 2021).

In a similar analysis of CO_2 emissions, Longden et al. (2022) compared emissions from hydrogen production using SMR, black and brown coal gasification (CG), and the use of black and brown coal and natural gas for heating. For this study, more favorable CO_2 capture rates were assumed; when capturing the emissions from the stream gas via SMR, the capture efficiency is 56%, whereas capturing emissions from both sources (the stream gas and the flue gas) improves the capture rate of CO_2 to 90%. However, the plant's overall energy efficiency is reduced from 74% to 69%, respectively, as more energy is required to run the capture equipment. For CG, the capture rate is assumed as 90%, and a plant energy efficiency of 63% (Longden et al., 2022, p. 4). Fugitive emissions rates for natural gas are taken from the IPCC, which is lower than the previous study by Howarth & Jacobson (2021). These rates are 1.7% (default) and 2.58% (highest value). For brown coal, default fugitive emissions are 1.21% (default) and 1.68% for low and high value, respectively. It also included the energy to compress the CO_2. However, the additional fuel required to transport and store the CO_2 is not included. Moreover, LHV is considered for this study (Longden et al., 2022, p. 4).

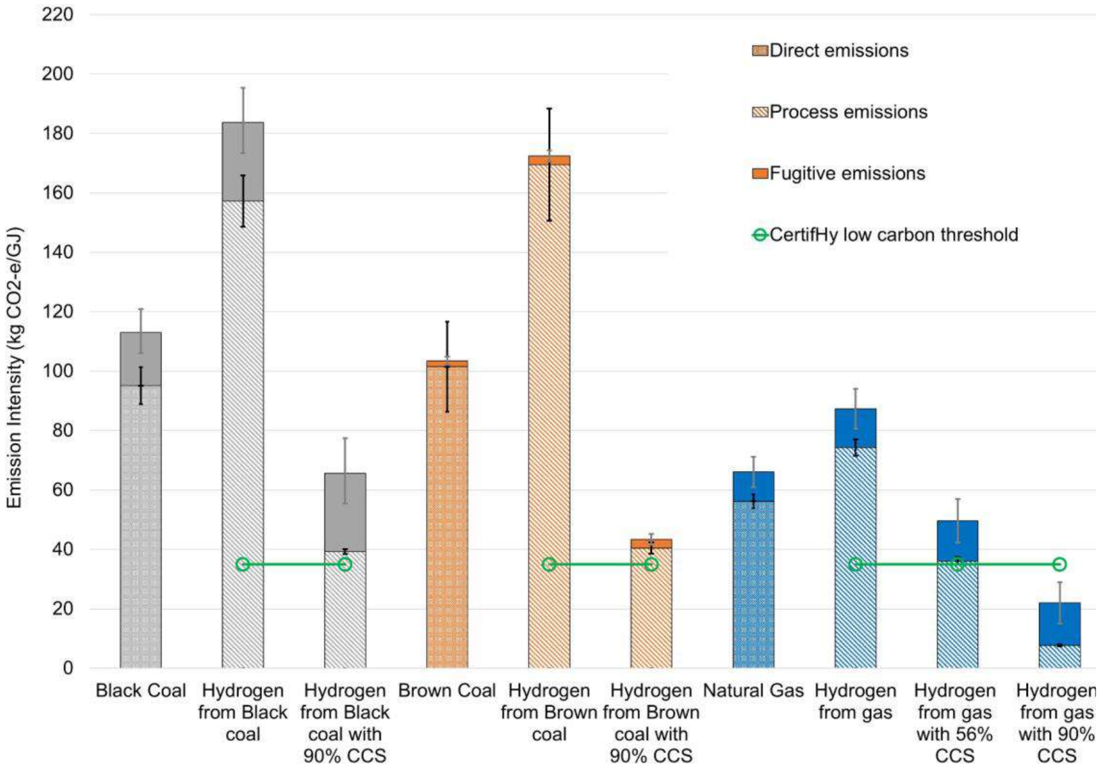

Figure 19. The total emission intensity of different fuels (Longden et al., 2022, p. 3).[8]

Figure 19 shows CO_2 emissions from different fuels using the author's model and assumptions mentioned above. Data is presented in $kgCO_2$ equivalent per unit of energy (GJ) equivalent to g $CO_{2\text{-eq}}$/MJ. The error bars in fugitive emissions represent the maximum and minimum values given by IPCC. Moreover, the error bars present indirect emissions, and process emissions are the maximum and minimum emissions due to natural variations in the carbon content of the different fuels. Results show that from the three methods to obtain blue hydrogen, SMR with a capture rate of 90% has the lowest CO_2 emissions in its life cycle of around 21 kg CO_2-e/GJ (21 gr CO_2-e/MJ) when the fugitive emission rate is 1.7% (Longden et al., 2022, p. 4). The CertiHy threshold line, a European certification scheme, indicates that a 60% reduction in emissions compared to standard SMR must be achieved to qualify as 'low carbon' hydrogen. According to that, only hydrogen from SMR with 90% CCS classifies as low emissions (Longden et al., 2022, p. 5).

Compared to the study by Howarth & Jacobson (2021) by a sensitivity analysis, Longden et al. (2022) assumed a 3.5% methane leakage rate and low and default

[8] Reprinted from Applied Energy, Vol 306, Thomas Longden, Fiona J. Beck, Frank Jotzo, Richard Andrews, Mousami Prasad, 'Clean' hydrogen? – Comparing the emissions and costs of fossil fuel versus renewable electricity based hydrogen, 118145, Copyright (2022), with permission from Elsevier.

IPCC leakage rates with GWP20 and GWP100 in their calculation, as shown in Table 11.

Table 11. Total emissions intensity (fugitive, process, and direct) using different methane leakage and 20 and 100-year global warming potentials (GWP) (Longden et al., 2022, p. 9).[9]

GWP and methane leakage rate (%) used	Natural gas	Hydrogen from gas	Hydrogen from gas with 56% CCS	Hydrogen from gas with 90% CCS
100-year GWP of 28				
0.9% (IPCC low)	61.25	80.19	43.60	15.6
1.7% (IPCC default)	65.92	87.06	49.47	22.35
3.5% (Howarth & Jacobson)	76.42	100.88	63.73	37.54
20-year GWP of 86				
0.9% (IPCC low)	72.13	95.23	59.33	31.33
1.7% (IPCC default)	86.46	114.11	77.37	52.06
3.5% (Howarth & Jacobson)	118.71	156.57	121.18	98.72

The model used by the authors using a GWP20 yielded a carbon intensity of 118.7 and 156.5 kg $CO_{2\text{-eq}}$/GJ (gr $CO_{2\text{-eq}}$/MJ) for burning natural gas and producing gray hydrogen, respectively (Longden et al., 2022, p. 9). It is similar to emissions of 111 and 153 kg $CO_{2\text{-eq}}$/GJ presented by Howarth & Jacobson (2021, p. 9) in Figure 18 when assuming a leakage rate of 3.5%. However, capture efficiencies were calculated differently in these two studies, being the ones in the latest work more optimistic (56 and 90% against 47 and 76%), yielding less carbon intensity (Howarth & Jacobson, 2021; Longden et al., 2022). Finally, the reduction in CO_2 emissions from blue hydrogen is between 23 to 36% lower with GWP20 and 3.5% methane leakage rate compared to gray hydrogen. However, it decreases when considering lower emission rates and a GWP100. Hydrogen from natural gas without CCS produces more CO_2 than burning natural gas in every scenario. Blue hydrogen with CCS 56%, 3.5% leakage rate, and GWP20 is an exception in which CO_2 intensity is slightly higher (Longden et al., 2022, p. 4). The authors conclude that by considering realistic CO_2 capture rates and fugitive emissions, blue hydrogen production yields significant GHG emissions (Longden et al., 2022, p. 9).

The publication titled ‘On the climate impacts of blue hydrogen’ by Bauer et al. (2022), claims that the work by Howarth & Jacobson (2021) had the opposite results in $CO_{2\text{-eq}}$ reductions from blue hydrogen compared to their previous publication. Therefore, their previous study showed that $CO_{2\text{-eq}}$ reductions are between 50-80%

[9] Reprinted from Applied Energy, Vol 306, Thomas Longden, Fiona J. Beck, Frank Jotzo, Richard Andrews, Mousami Prasad, ‘Clean’ hydrogen? – Comparing the emissions and costs of fossil fuel versus renewable electricity based hydrogen, 118145, Copyright (2022), with permission from Elsevier.

for blue hydrogen compared to gray hydrogen with standard SMR without CCS and GWP100 (Antonini et al., 2020).

Thus, Bauer et al. (2022) investigated this contradiction in another study. The methodology of this study relies on three aspects when producing blue hydrogen: the chosen technology, fugitive methane emissions, and global warming potential metrics (GWP). Following these three aspects and the study by Antonini et al. (2020) the LCA model considers two blue hydrogen plant configurations; SMR with a 90% capture rate (CCS-low) and ATR (auto-thermal reforming) with a 98% capture rate (CCS-high). Both configurations capture CO_2 from the process gas. Therefore, overall plant-wide CO_2 capture is reduced to 55% for SMR, as CO_2 from the flue gas is not captured, and 93% for ATR. Even though ATR does not have a combustion chamber, a small fire heater emits CO_2. This previous study also demonstrated that some hydrogen plant configurations produce excess electricity, which can be used to replace the required electricity (from the average grid) during the process (Bauer et al., 2022, p. 72). As this study is based on a hydrogen plant in Europe that produces nine tons/h, the electricity supply corresponds to the ENTSO-E[10] database, and a methane emissions average rate of 1.3% from natural gas supplied to the European countries (the German institution ifeu[11] verified the value). However, this methane emissions rate is modified according to the values reported in different countries to 0.2% (Norway, the UK, and the Netherlands), 1.5% (medium value), and 8% (Libya and the US). These values allowed the study to cover a better range of emissions. Methane emissions from high-pressure pipelines are included as they deliver natural gas to the production plant. The authors maintained all other additional variables constant, such as CO_2 from natural gas flaring, energy demand for compression of natural gas, and the need for transportation infrastructure represent an additional 9 to 10 gCO_2-eq for GWP20 and GWP100, respectively (Bauer et al., 2022, pp. 72–73). Moreover, the LCA model includes emissions for transporting CO_2 through a 200 km pipeline from the production plant to the storage formation (saline aquifer) with a depth of 1 km (Bauer et al., 2022, p. 73), which were missing in the studies made by Howarth & Jacobson (2021) and Longden et al. (2022) mentioned above. However, results from variating these distances and depths do not significantly impact LCA analysis (Bauer et al., 2022, p. 73).

[10] ENTSO-E, the European Network of Transmission System Operators for Electricity, is the association for the cooperation of the European transmission system operators (TSOs). https://www.entsoe.eu/about/inside-entsoe/objectives/

[11] Institut für Energie- und Umweltforschung https://www.ifeu.de/en/institute/how-we-see-ourselves/

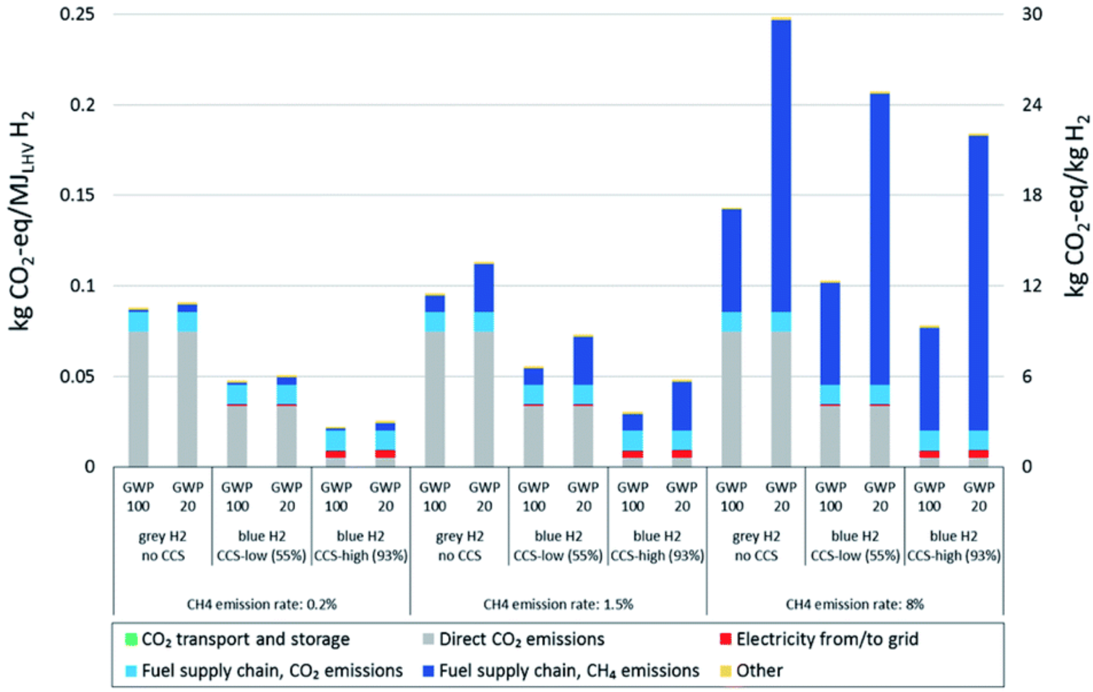

Figure 20. Impacts on climate change are associated with the production of NG-based hydrogen (Bauer et al., 2022, p. 69).

Results from the study are presented in Figure 20. Blue hydrogen production yields less CO_2 than gray hydrogen in GWP20 and GWP100 in every given scenario. Direct methane emissions and emissions from the supply chain are constant for every technology and GWP. However, methane leakage rate plays an important role when calculating impacts on climate change in both $kgCO_{2\text{-}eq}/MJ_{LHV}H_2$ and $kgCO_{2\text{-}eq}/kgH_2$. Reductions of $CO_{2\text{-}eq}$ emissions achieved with blue hydrogen compared to gray hydrogen are more noticeable with lower methane leakage rate and are not representative in both GWP20 and GWP100. However, the higher the leakage rate, the lower the reduction and the more significant the difference between global warming potentials (Bauer et al., 2022, p. 70). Table 12 (Bauer et al., 2022, p. 70) shows this reduction in percentage.

Table 12. Reduction of GHG emissions. Own table based on Bauer et al. (2022, p. 70).

	Leakage CH_4 rate 0.2%		**Leakage CH_4 rate 8%**	
	Gray H_2	Blue H_2	Gray H_2	Blue H_2
GWP20	100	72	100	26
GWP100	100	75	100	45

The authors conclude that blue hydrogen could become close to green hydrogen when low GHG emissions are controlled and minimized during the entire supply chain of natural gas. Second, the appropriate technology to produce hydrogen must integrate CO_2 capture in the planning stage to reduce additional energy demand. Third, the use of global warming potential metrics gains importance when methane leakage rates are high, and the impact of these emissions is analyzed in the short to midterm (2050), being GWP20 more relevant in this scenario (Bauer et al., 2022, p. 71).

In a more recent study included in this thesis and following the analysis by Antonini et al. (2020), Schippert et al. (2022) developed an in-depth analysis using a new model with natural gas data from Europe and two different transport options. The first option includes a hypothetical production of hydrogen in Germany with imported natural gas from a 4000 km pipeline and delivery of hydrogen with a 300 km pipeline referred to as 'natural gas import'. As a second option, the distances are inverted; hydrogen is produced from a 300 km natural gas pipeline, then imported by Germany from a 4000 km pipeline. Hence, it is referred to as 'hydrogen import'. The global warming potential is taken from IPCC, which is 81.2 ($kgCO_{2-eq}$) for methane and 1 for CO_2 with GWP20 (Schippert et al., 2022, pp. 4–5).

For this study, the life cycle assessment (LCA) was calculated taking into account the following steps: production and transport of natural gas, hydrogen production, transportation and storage of CO_2, and hydrogen transport to the end customers. For this calculation, six different hydrogen processes were considered (Table 13) (Schippert et al., 2022, p. 4).

Table 13. Hydrogen process options with and without CCS. Own table based on Schippert et al. (2022, pp. 5, 14).

H_2 process	Water Gas Shift (WGS)	CCS	% CCS	Referred as
SMR	High temperature (HT)	No	0	SMR / no CCS
SMR	High temperature (HT)	Via Amines	55	SMR / low CCS
SMR	High temperature, low temperature (HTLT)	Via VPSA	70	SMR / high CCS
ATR	HTLT	No	0	ATR / no CCS
ATR	HTLT	Via Amines	86	ATR / low CCS
ATR	HTLT	Via VPSA	98	ATR / high CCS

The authors took mean values from European institutions[12] to calculate methane and CO_2 emissions from natural gas production and transport. They found that many consumers get natural gas from secondary networks operating at lower pressure. In this case, emissions are taken as constant values. On the other hand,

[12] Zukunft ERDGAS GmbH, DBI Gasund Umwelttechnik GmbH, the European Commission DG ENER.

in high-pressure transport networks, apart from leaks, emissions from natural gas transport increase with distance since it is necessary to power the compressors to maintain the pressure in the pipelines. That means the longer the length, the more emissions are accounted for (Schippert et al., 2022, p. 3). Different from previous studies, this study performs an in-depth analysis by taking more variables into account than the studies by Bauer et al. (2022), Howarth & Jacobson (2021), and Longden et al. (2022). Table 13 shows selected hydrogen production technologies and carbon capture efficiencies based on the work from Schippert et al. (2022). In addition, the authors included indirect emissions from producing the amine (MEA), which degenerates when capturing the CO_2 by chemical adsorption. On the other hand, carbon capture through vacuum pressure swing adsorption (VPSA) does not require MEA. Thus, no emissions for its production are associated (Schippert et al., 2022, p. 3).

Moreover, indirect emissions for transporting and storing CO_2 are possible leakages and electricity to power the compressors, which are assumed to be from the grid as there is no fuel (natural gas or hydrogen) to power them. However, the pressure to inject CO_2 underground is higher than the one required for transport. Thus, more electricity is needed (Schippert et al., 2022, pp. 3–4). The study states how challenging it is to predict the average leakage rate of final disposal sites underground because permanent CO_2 disposal on a big industrial scale is still relatively new. Therefore, it considers the IPCC's premise that during 1000 years, less than 1% of the stored CO_2 will leak into the atmosphere is considered (Schippert et al., 2022, p. 4).

The research includes the final stage of the LCA, the transport of hydrogen from the production site to the potential customer. It follows the same pipeline system for natural gas and CO_2 transportation. In this scenario, hydrogen is used to power the compressors to compensate for the pressure due to losses. The authors assume no GHG emissions from burning hydrogen. Thus, only indirect emissions from the production of the additional hydrogen that is burned to deliver a specific quantity of hydrogen to the customers are considered (Schippert et al., 2022, p. 4). Furthermore, blue hydrogen production requires resources to build the necessary infrastructure in which indirect emissions are included in the hydrogen production stage. Therefore, the study does not consider emissions from the natural gas network infrastructure, as they already exist. In contrast, emissions from building

CCS facilities, transport, and storage of CO_2, and hydrogen transport are considered (Schippert et al., 2022, p. 4).

The total emissions in $kgCO_{2-eq}/kgH_2$ are presented in 12 different scenarios in Figure 21. These scenarios are a combination of the six hydrogen production processes (see Table 13) and the two possible locations of the hydrogen production plant and subsequent transport (natural gas import and hydrogen import) (Schippert et al., 2022, pp. 5–6). From this figure, it is inevitable that distance is significant and does affect the total GHG emissions. Results of this study indicate that using methane reforming with either SMR or ATR does not have a difference in GHG emissions when CCS is not coupled. Moreover, ATR can remove more emissions than SMR as it can have a higher carbon capture rate. Therefore, the location of the production plant, carbon capture rate, and natural gas reforming technology influence the total emissions when producing blue hydrogen (Schippert et al., 2022, p. 6).

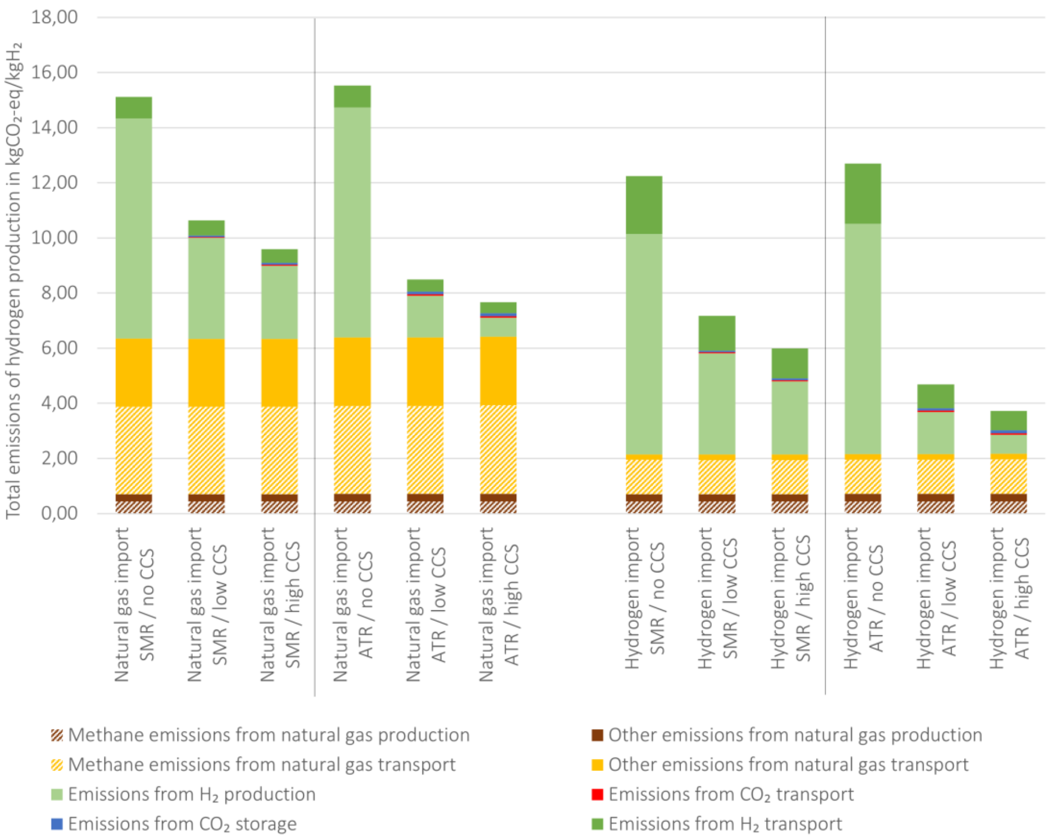

Figure 21. Results of life cycle assessment of hydrogen production with transportation distances of 4000 km for natural gas and 300 km for hydrogen (scenario natural gas import) respective 300 km for natural gas and 4000 km for hydrogen (scenario hydrogen import) (Schippert et al., 2022, p. 6).

The study classifies the sources of GHG emissions according to the life cycle assessment results. The sources are organized according to their relevance in Table 14 (Schippert et al., 2022, p. 6).

Table 14. Classification of emission source. Own table based on Schippert et al. (2022, p. 6).

CO_2 emissions	Process step
Major source	Natural gas transport Hydrogen production
Medium source	Natural gas production Hydrogen transport
Minor relevance	CO_2 transport and storage
Insignificant	Construction of infrastructure

The authors conclude that upstream natural gas emissions are the main source of GHG emissions in the whole supply chain to produce blue hydrogen. Therefore, they focus on reducing the transport distance of natural gas to reduce emissions by, ideally, producing natural gas and hydrogen in the same location. However, despite a significant reduction of emissions when CCS is included, they also note that total $CO_{2\text{-eq}}$ emissions from producing blue hydrogen are still substantial compared to green hydrogen production (Schippert et al., 2022, p. 8).

In conclusion, previous studies analyzed blue hydrogen production, which calculated $CO_{2\text{-eq}}$ emissions through different models and assumptions. These calculated emissions determine whether blue hydrogen is a low-carbon alternative and can play an essential role in helping decarbonize current hydrogen applications. Therefore, its environmental impact is assessed through life cycle assessments (LCA).

All mentioned authors agree that upstream emissions for producing and transporting natural gas and direct process emissions from the gas reforming (no CCS included) are the main contributors to the overall calculation of CO_2 emissions. They also agree that there is currently no CCS technology able to capture the total CO_2 emissions from the process in both SMR and ATR, as the carbon capture efficiency is still under 100% (Bauer et al., 2022; Howarth & Jacobson, 2021; Longden et al., 2022; Schippert et al., 2022). The different LCA shows that burning natural gas for heating could produce less $CO_{2\text{-eq}}$ emissions than gray hydrogen (Bauer et al., 2022; Longden et al., 2022) or even some blue hydrogen configurations (Howarth & Jacobson, 2021).

Different Technology options were explored in these studies. The SMR technology was compared without CCS and with CCS and two different carbon capture rates; the higher the capture rate, the better (Howarth & Jacobson, 2021). Other studies elaborate on comparing SMR and ATR, finding the last one the better option (Bauer et al., 2022; Schippert et al., 2022). Regarding feedstock, coal gasification and SMR were compared, proving that replacing natural gas with coal produces more $CO_{2\text{-eq}}$ emissions in most of the analyzed scenarios (Longden et al., 2022). While emissions from the transport and storage of CO_2 are not included in some models (Howarth & Jacobson, 2021; Longden et al., 2022), results after having them are not representative of the overall total emissions (Bauer et al., 2022; Schippert et al., 2022). However, data from CO_2 transport and storage is not well known and was assumed (Schippert et al., 2022). Furthermore, emissions from hydrogen transport are only included as indirect emissions for producing the required additional hydrogen, stating that there are no direct GHG emissions from burning hydrogen (Bauer et al., 2022).

Figure 22 compares the climate impact of producing gray and blue hydrogen in gCO_2/MJ_{H2} according to the studies mentioned above in this thesis. This comparison takes the calculations with a global warming potential of 20 (GWP20) for short-term climate impact.

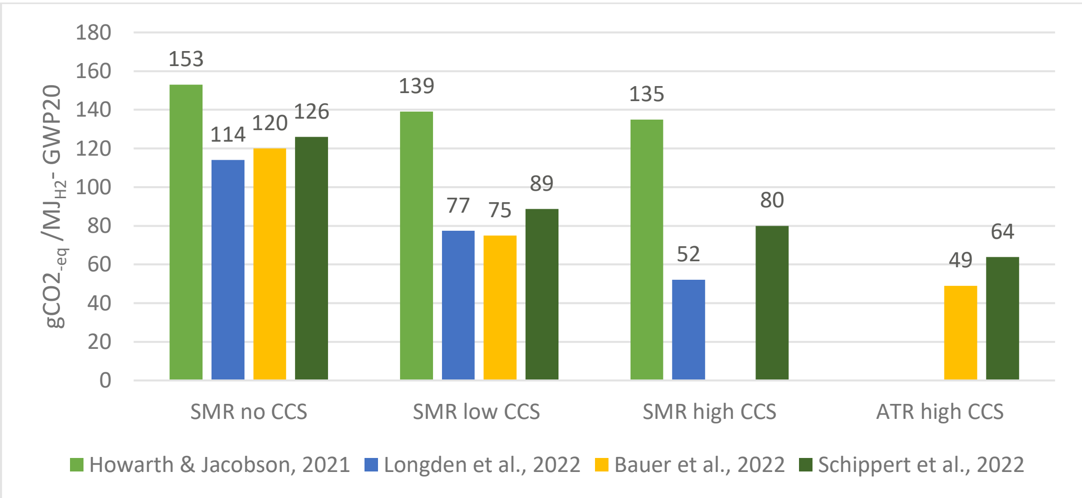

Figure 22. Comparison between studies of the total CO2-eq emissions for gray and blue hydrogen production technology with a GWP20. Own figure based on Bauer et al. (2022); Howarth & Jacobson (2021); Longden et al. (2022); Schippert et al. (2022).

It is worth noting that not all studies consider the same scenarios and parameters. Thus, total $CO_{2\text{-eq}}$ emissions vary among them. It can be seen how the results after the initial research by Howarth & Jacobson (2021) yield lower values, which are still significant when talking about GHGs and climate change. The results show that data needs to be standardized, and there is no agreement on how emissions should be calculated to deploy green and blue hydrogen in the upcoming decades.

4.3. Efficiency and Cost of Green and Blue Hydrogen

Current net efficiencies in energy content (LHV) of gray hydrogen are between 76-77% of the natural gas used as a feedstock for SMR and ATR (Bauer et al., 2022). Nikolaidis & Poullikkas (2017) compared the efficiency of SMR (74-85%), ATR (60-75%), POX (60-75%), and electrolysis (40-60) in Table 4. Braga et al. (2017b, p. 123) compared the efficiencies of electrolysis from hydropower (close to 80%), followed by SMR efficiency of around 70%, and electrolysis from wind and solar PV at the end at 30% and 10%, respectively.

In terms of average costs, in most of the world's regions, creating hydrogen from fossil fuels is currently the least expensive alternative. The Levelized cost of producing hydrogen from natural gas ranges from USD 0.5 to USD 1.7 per kilogram. The Levelized cost of production rises to about USD 1 to 2 per kilogram when CCUS is added to cut CO_2 emissions. Hydrogen production with renewable electricity ranges from USD 3 to 8 per kg (IEA, 2021a, p. 7).

By 2050, the International Energy Agency (IEA) estimates that blue hydrogen cost will fall to USD 1-2 per kg, depending on the natural gas cost, ranging from 15 to 55% of the total cost. Green hydrogen via water electrolysis would benefit from scaling up the technology, reducing the hydrogen cost per kg from USD 1.5 to 3 in 2030 to USD 1 to 2.5 in 2050. In this case, the cost varies depending on the cost of renewable electricity (IEA, 2021b, p. 110).

4.4. Future Hydrogen Demand

Global hydrogen demand is expected to grow in the short-term (2030) and long-term (2050) scenarios. It is expected that Australia, Latin America, and the Middle East will be the hydrogen producers to supply demand to Europe, the Western US, Japan, and Korea (Hydrogen Council, 2021, p. 14).

The International Energy Agency (IEA), in the ‘Net Zero by 2050’ report, focuses on using low-carbon hydrogen (coal and natural gas with CCUS and electrolysis) in existing uses such as refineries, industry, and power plants where there is no immediate need to replace current infrastructure for transmission and distribution. In this scenario Figure 23, hydrogen demand will grow from almost 90 Mt to 212 Mt in

2030 and 528 Mt in 2050. As a result, shares of low-carbon hydrogen will also increase from around 70% in 2030 to 98% in 2050. (IEA, 2021b, pp. 75–76).

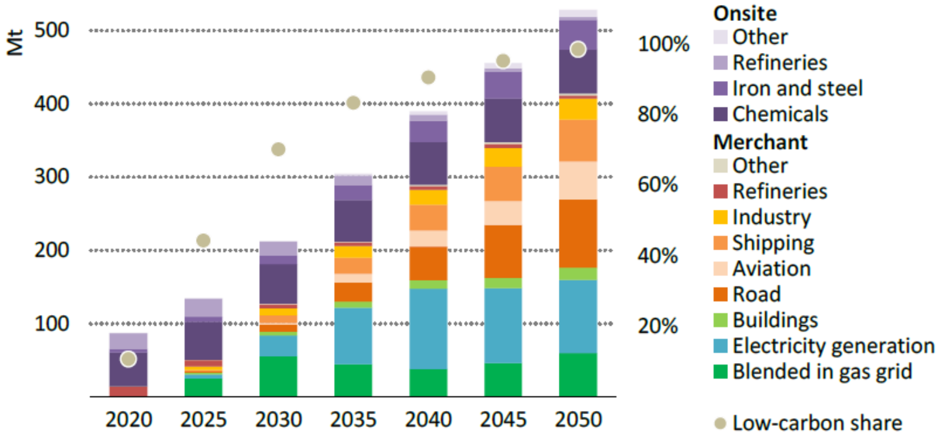

Figure 23. Global hydrogen demand in the NZE (IEA, 2021b, p. 75).

According to this report, by 2030, advancements should make it possible to quickly scale up the production of electrolyzers and create new hydrogen transportation infrastructure simultaneously. The authors state that this should cause cost reductions for electrolyzers and hydrogen storage, particularly in salt caverns. Furthermore, the imbalance between hydrogen demand and its supply by off-grid renewable energy sources and seasonal variations in power demand are countered by stored hydrogen. According to IEA, hydrogen and ammonia (hydrogen-based fuel) use will expand to electricity generation in co-fired plants with natural gas and coal, respectively, by 2050. Moreover, blended natural gas with 15% hydrogen is used in gas networks. In transport, depending on policy-makers decisions by 2030, almost one-third of the fuel used in trucks is hydrogen. Moreover, around 60% of fuel demand in shipping is supplied by hydrogen-based fuels (IEA, 2021b, pp. 75–76).

A similar approach is taken by the Hydrogen Council[13], which agrees in its 'Hydrogen for Net Zero' publication that hydrogen's primary role is in cost-efficiently decarbonizing sectors that are hard to electrify. According to Figure 24, the report estimated a total hydrogen demand of 140 Mt in 2030 and 660 Mt in 2050 (Hydrogen Council, 2021, p. 13).

[13] The Hydrogen Council is a think tank formed in 2017 by industry, namely British Petroleum, Shell and other oil and gas majors.

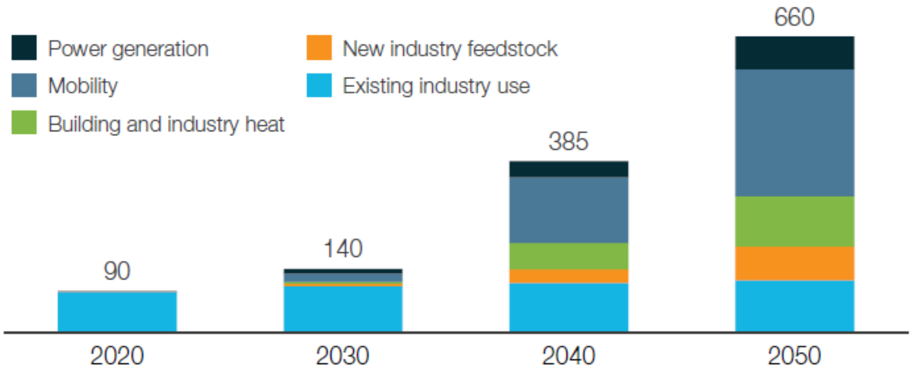

Figure 24. Global hydrogen demand by segment until 2050 (Hydrogen Council, 2021, p. 13).

The authors stated that accelerating hydrogen deployment by 2030 is essential to achieve 2050 temperature goals. In this scenario, 75 Mt out of 140 Mt comes from clean hydrogen (low-carbon and renewable hydrogen). It is necessary to convert 25 Mt of gray hydrogen plus 50 Mt of clean hydrogen to achieve a total of 75 Mt. From current demand, there will be a moderate increase in ammonia and methanol production and refining. Moreover, significant growth in new industrial uses for steelmaking via DRI and overall mobility is expected. Power generation will be primarily driven by blending hydrogen with natural gas in turbines and coal power plants blended with ammonia. Blended natural gas with hydrogen for residential use and the development of high-grade industrial heating will be in the early stage (Hydrogen Council, 2021, p. 13). The report concluded that depending on policies, such as high carbon prices, to support the gray hydrogen phase-out, only clean hydrogen will be produced in 2050. It is expected to supply demand in ammonia and steel production, direct use of hydrogen and hydrogen-based fuels in mobility (ground, maritime, and aviation), high-grade industrial applications and residential heating, power generation for seasonal balancing (storage) and power backup, and BTX (benzene, toluene, and xylene) production (Hydrogen Council, 2021, p. 13).

The International Renewable Energy Agency (IRENA), in its 1.5 °C scenario, considers only clean hydrogen production, which is low carbon from natural gas with CCS (blue hydrogen) and electrolysis using renewable electricity (green hydrogen). According to this report, clean hydrogen production will grow from 0.8 Mt in 2020 to 154 Mt in 2030 and by fourfold in 2050 to 614 Mt (see Figure 25) (IRENA, 2022a, p. 32, 2022b, p. 94).

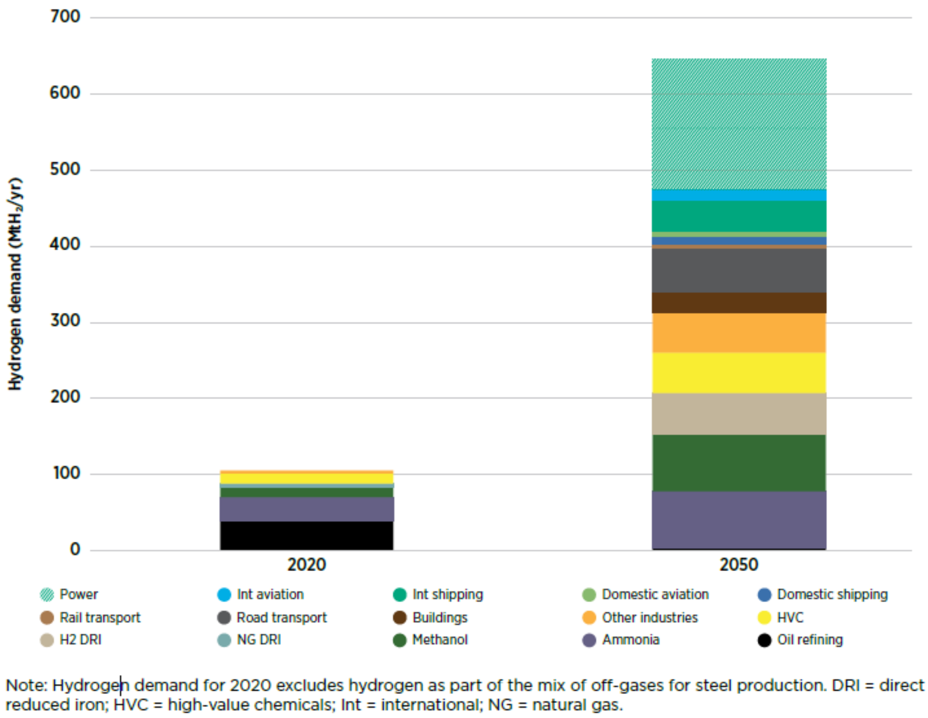

Figure 25. Hydrogen demand by application in 2020 and 2050 (IRENA, 2022a, p. 32).

The main target for using hydrogen, also mentioned by the other authors, is to offer a solution to mitigate emissions in hard-to-electrify sectors such as industry and transport directly. It highlights the importance of hydrogen in steel production through DRI and in the chemical and petrochemical industries. Moreover, it mentions the role hydrogen can play in balancing short-term fluctuations of renewable electricity and long-term flexibility between seasons through storage. It is also expected to play a minor role in providing complementary energy for buildings using the existing gas grid. However, policies are needed to promote hydrogen use through national strategies, setting sectoral priorities, certification systems to track lifecycle emissions, and incentives to switch from gray to green hydrogen, among others (IRENA, 2022a).

Yusaf et al. (2022) developed four scenarios for predicting hydrogen demand from 2021 to 2050 in their paper, considering two pathways of hydrogen use: fuel cells and combustion. Results in this report indicate that the combustion pathway may have consequences of successfully deploying hydrogen as it produces NO_x (an air pollutant). The first scenario consists of keeping current production levels to yield the lowest demand by 2050. The second one holds the current growing trend excluding 2020 due to the Covid pandemic and assuming no drastic changes. In the third scenario, the average growth of the last ten years is taken. Finally, in the last and best-case scenario, hydrogen is assumed to be the fuel of choice for the following applications: ammonia production, heavy and long-distance transportation, and backup capacity for grid power supply (Yusaf et al., 2022). According to the four scenarios presented in this study, Figure 26 shows that hydrogen demand can range from 73 Mt (2019) to 568 Mtn in 2050 (Yusaf et al., 2022, p. 11).

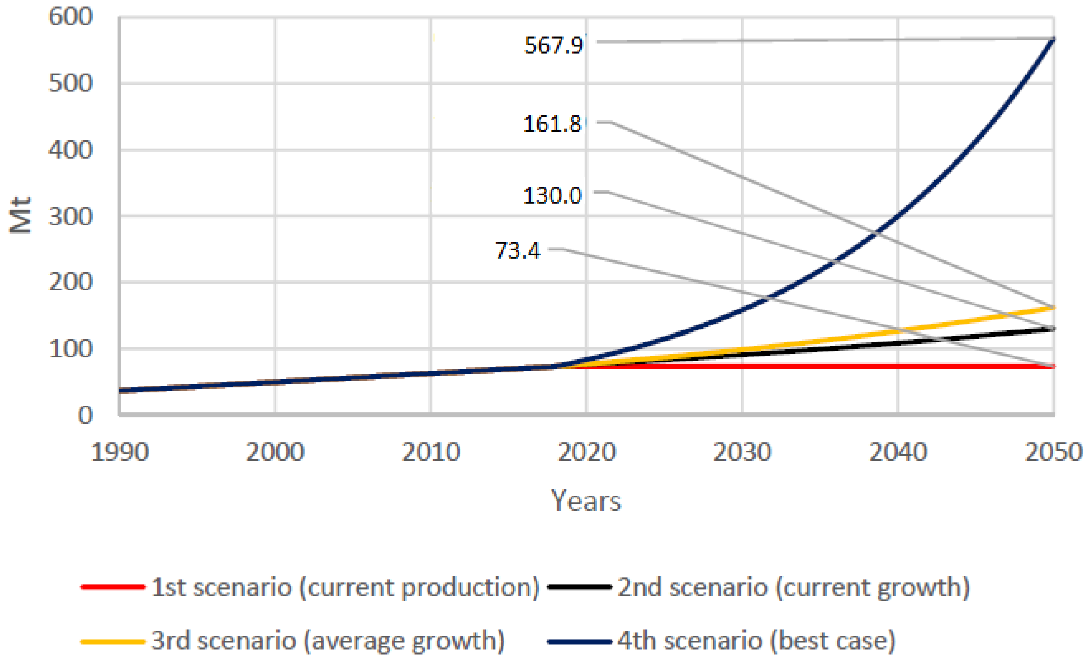

Figure 26. The potential global hydrogen demand. Adapted from Yusaf et al. (2022, p. 11).

In conclusion, the authors agreed that renewable and low-carbon hydrogen plays a significant role in first decarbonizing ammonia production, refining, steel industries, and long-distance transport. Followed by electricity generation as a backup and co-fired in power plants. However, hydrogen for heating in industrial processes and buildings is believed to play a minor role in decarbonizing these sectors in the long term. Figure 27 shows the expected hydrogen demand from the abovementioned sources. From these reports, the target is clear; it is needed between 528 to 660 Mt hydrogen in 2050 to supply the growing demand. However, a variation in demand of around 130 Mt is shown as it might be related to the final use of hydrogen in some sectors, such as heating in buildings and industrial processes and combustion for electricity production due to additional air pollutants.

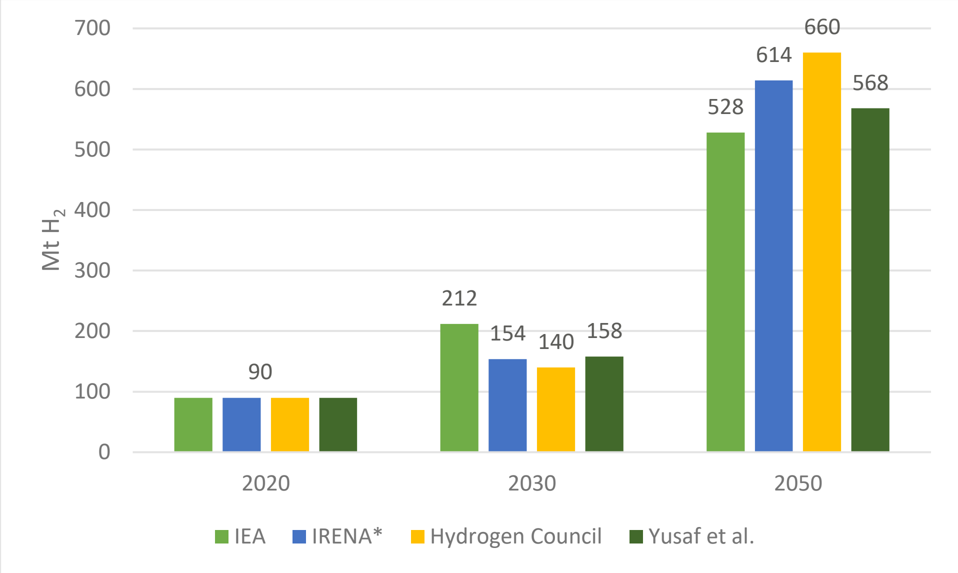

Figure 27. Comparison of future hydrogen demand according to different reports. *IRENA only considers the demand for clean hydrogen. Own figure based on Hydrogen Council (2021, p. 13); IEA (2021b, p. 76); IRENA (2022b, p. 94); Yusaf et al. (2022, p. 1).

According to these reports, it is certain that in the short-term green hydrogen will not be able to supply the growing demand by itself. Therefore, phasing-out gray hydrogen in industries where it is being used today is a priority, and blue hydrogen is there to balance the supply chain. In contrast, green hydrogen reaches total capacity to supply demand in the long term.

4.5. National Hydrogen Strategies

To meet this future hydrogen demand, governments worldwide are presenting their national strategies to include hydrogen and its products in their energy mix for importing and exporting. As of 2022, 26 governments have implemented a hydrogen strategy in their energy mix (IEA, 2022b). Based on the path toward hydrogen production, the national strategies can be classified into two groups (Longden et al., 2022). Some of these countries are shown in Table 15.

Table 15. Countries with national hydrogen strategies. Adapted from Longden et al. (2022, p. 2).[14]

Countries with national hydrogen strategies	
Prioritizes 'Zero-emission' H_2 (Green hydrogen is a priority)	**'Zero-emission' H_2 prioritized but 'low-emission' H_2 discussed as a transitional measure (Green hydrogen is a priority, but blue hydrogen plays a transitional role)**
Chile France New Zealand Portugal Spain	**Australia** **Canada** **China** **Colombia** **European Union** **Germany** **Japan** **Netherlands** **Norway** **Republic of Korea** **United States**

Longden et al. (2022) analyzed the strategies and found that there still needs to be a global consensus around a single favored technology strategy. Therefore, many nations will likely pursue strategies for increasing hydrogen production and continue to rely on fossil fuels. They concluded that if the industry is supported to travel down the road of reducing emissions, as suggested by how this decision is framed in national policies, there is a genuine risk that emissions in practice will be greater than predicted in such papers (Longden et al., 2022).

One example is Colombia and its national hydrogen strategy released in 2021. It considers using natural gas and coal to produce low-emission hydrogen with CCUS since this country has significant coal and natural gas reserves. They also mentioned that CO_2 emissions for blue hydrogen have an emissions intensity below 2 kg CO_2/kgH_2 (Ministerio de Minas y Energía, 2021, p. 5), which is significantly low compared to the values presented in section 4.2. However, during the first stage of development, part of the electricity for water electrolysis will be supplied by the grid as the Colombian electricity mix comes mostly from hydropower. Thus, the emissions intensity was estimated to be around 8 kg CO_2/kgH_2 (Ministerio de Minas y Energía, 2021, p. 6), which is considerably low, compared to electrolysis using the average electricity grid from the US and EU presented in Figure 17.

[14] Reprinted from Applied Energy, Vol 306, Thomas Longden, Fiona J. Beck, Frank Jotzo, Richard Andrews, Mousami Prasad, 'Clean' hydrogen? – Comparing the emissions and costs of fossil fuel versus renewable electricity based hydrogen, 118145, Copyright (2022), with permission from Elsevier.

5 Results

This chapter assesses the climate impact on $CO_{2\text{-eq}}$ emissions of gray, blue, and green hydrogen production that will supply future demand. To do so, two research models previously described in section 4.2 and two future hydrogen demand scenarios described in section 4.4 will be used to calculate the $CO_{2\text{-eq}}$ emissions when producing gray, green, and blue hydrogen. To calculate the $CO_{2\text{-eq}}$ emissions from two future hydrogen demand estimates, six scenarios with low and high carbon capture rates from two studies have been selected. These calculations consider short-term (2030) and long-term (2050) emissions. These results will then be used to analyze the climate impact of currently available technologies in different scenarios intended to supply the estimated future hydrogen demand.

5.1. Selection of Hydrogen Production Methods

Following the comparison of blue hydrogen production methods in Figure 22, two studies were selected: the first study, referred to as 'Study 1' in this thesis, is from Howarth & Jacobson (2021). The authors obtained the highest value of $CO_{2\text{-eq}}$ emissions per MJ_{H2}. The authors performed the calculation using Higher Heating Values (HHV) and data from the U.S. Hence, they concluded that blue hydrogen does have a significant climate impact, and this led to the conduction of other studies mentioned in section 4.2 (Bauer et al., 2022; Longden et al., 2022; Schippert et al., 2022). The second study referred to as 'Study 2' by Schippert et al. (2022), included additional variables in the model, such as natural gas transport distance, CO_2 transport and storage, construction of infrastructure, and hydrogen compression and transport with data from Europe and the used of Lower Heating Values (LHV). Results of $CO_{2\text{-eq}}$ emissions from this study are slightly higher than those from Bauer et al. (2022) and Longden et al. (2022) and lower than those from Howarth & Jacobson (2021).

The best and worst-case scenarios in terms of CO2-eq emissions from each study are considered for the analysis. The best-case scenario from Howarth & Jacobson (2021) is the production of blue hydrogen via SMR with a carbon capture rate of 76% (Own calculation based on Howarth & Jacobson (2021, p. 5)). From Schippert et al. (2022, p. 14), hydrogen production via ATR with a carbon capture rate of 98% was selected. On the other hand, the worst-case scenario in terms of high $CO_{2\text{-eq}}$ emissions from each model is the following: production of blue hydrogen via SMR and a carbon capture rate of 47% (Own calculation based on Howarth & Jacobson (2021)) and hydrogen production via SMR and a carbon capture rate of 55%

(Schippert et al., 2022, p. 14). ‘Study 3’ represents de hydrogen production entirely through water electrolysis and will be described below. Apart from that, a fourth study, referred to as ‘Study 4’ by Schippert et al. (2022), in which the natural gas transport distance (300 km) is shorter than the hydrogen transport distance (4000 km) is included. This fourth study is interesting because less $CO_{2\text{-eq}}$ / kgH_2 is produced than in ‘Study 1’ and ‘Study 2’. Thus, blue hydrogen production via SMR with a carbon capture rate of 55%, ATR with a carbon capture rate of 98%, and gray hydrogen production via SMR were selected (Schippert et al., 2022). ‘Study 4’ will be analyzed separately as it has different variables than ‘Study 1’ and ‘Study 2’. In all scenarios, $CO_{2\text{-eq}}$ emissions from gray hydrogen production via SMR are included for comparison purposes. Gray hydrogen via ATR yields almost the same CO_{2eq} emissions (Schippert et al., 2022). Therefore, only $CO_{2\text{-eq}}$ emissions from gray hydrogen via SMR are included. All blue hydrogen studies use GWP20 and GWP100 to calculate $CO_{2\text{-eq}}$ emissions to show the climate impact in the short term and in the long term, respectively. For green hydrogen, only results with GWP100 were found in the literature. The study by Howarth & Jacobson (2021) presents the $CO_{2\text{-eq}}$ emissions in g $CO_{2\text{-eq}}$/MJ, which was converted to kg $CO_{2\text{-eq}}$/kgH_2 using 143 MJ/kgH_2 (HHV) according to Table 3. Data from Schippert et al. (2022) was already in kg $CO_{2\text{-eq}}$/kgH_2. The selected studies and values are summarized in Table 16.

Table 16. Selected methods for blue hydrogen production. Own table based on Howarth & Jacobson (2021); Schippert et al. (2022).

H_2 process	% CCS	g CO2-eq / MJ	kg CO2-eq / kgH_2 GWP20	kg CO2-eq / kgH_2 GWP100	Referred to as
SMR	0	153	21.88	15.16	Study 1 / no CCS
SMR	47	139	19.88	12.30	Study 1 / low CCS
SMR	76	135	19.31	11.01	Study 1 / high CCS
SMR	0	-	15.11	12.50	Study 2 / no CCS
SMR	55	-	10.64	8.10	Study 2 / low CCS
ATR	98	-	7.66	5.00	Study 2 / high CCS
SMR	0	-	12.10	11.00	Study 4 / no CCS
SMR	55	-	7.10	5.90	Study 4 / low CCS
ATR	98	-	3.8	2.70	Study 4 / high CCS
For Study 1, 143 MJ/kg (HHV) were used to convert in kg CO2-eq / kgH_2. Study 2 uses 120 MJ/kg (LHV)					

For green hydrogen production via water electrolysis using wind and solar PV electricity (Study 3), the mean values of $CO_{2\text{-eq}}$ emissions were calculated using data from (Valente et al., 2017). Mean values of $CO_{2\text{-eq}}$ emissions from water electrolysis using wind and solar PV electricity were taken from 28 harmonized cases (19 wind and 9 Solar PV)(Valente et al., 2017, p. 770). For this thesis, the calculated wind-solar average emissions of 1.83 kg $CO_{2\text{-eq}}/kg_{H2}$ from Table 9 will be referred to in 'Study 3'. Table 17 summarizes each production method's highest and lowest value and the calculated average.

Table 17. CO_2 emissions from green hydrogen. Own table based on Valente et al. (2017, p. 770).

Green H_2 Process	kg CO2-eq / kgH_2
Wind high	2.29
Wind average	0.94
Wind low	0.16
Solar High	7.54
Solar average	3.7
Solar low	0.69
Wind-Solar average (Study 3)	1.83

5.2. Selection of Scenarios for Future Hydrogen Demand

According to section 4.4, hydrogen demand is expected to grow, and it will be supplied by a mix of green, blue, and gray hydrogen in the short and long term. Figure 27 compares the proposed hydrogen demand of four different reports (Hydrogen Council, 2021; IEA, 2021b; IRENA, 2022b; Yusaf et al., 2022). Two future hydrogen demand scenarios were selected to calculate the total $CO2_{\text{-eq}}$ emissions of gray, blue, and green hydrogen production and the shares of each in 2030 (short term) and 2050 (long term). The International Renewable Energy Agency (IRENA) report does not specify the percentage of gray hydrogen in its estimated demand; it only mentions blue and green hydrogen. The study by Yusaf et al. (2022) does not include the share of gray, blue, and green hydrogen. Thus, the International Energy Agency (IEA) and The Hydrogen Council (THC) estimates were chosen because they offer a complete future hydrogen estimate.

According to Figure 27, the IEA estimates a hydrogen demand of 212 Mt by 2030, which is higher than the estimates from the other three reports, with THC having the lowest value of 140 Mt. By 2050, the estimates are reversed, and the IEA estimates the lowest value with 528 Mt and The Hydrogen Council with 660 Mt the highest value (Hydrogen Council, 2021; IEA, 2021b). Therefore, the highest and lowest estimates of each report will be used to calculate the $CO2_{\text{-eq}}$ emissions and analyze the climate impact in the short and long term. Table 18 summarizes the selected future hydrogen demands included in this analysis.

Table 18. Future hydrogen demand in 2030 and 2050. Own table based on Hydrogen Council (2021); IEA (2021b).

Institution	Term (year)	Demand (MtH_2)	Referred to as
IEA	2030	212	IEA2030
IEA	2050	528	IEA2050
THC	2030	140	THC2030
THC	2050	660	THC2050

To be more specific, every report estimates the share of gray, blue, and green hydrogen in the short and long-term demand. Total hydrogen demand values and percentages are taken from the reports mentioned in section 4.4 (Hydrogen Council, 2021; IEA, 2021b). In its 2050 scenario, the Hydrogen Council estimates that low carbon hydrogen supply would be between 20-40%, whereas renewable hydrogen supply would be between 60-80% (Hydrogen Council, 2021, p. 19). Thus, an average of 30% for low-carbon hydrogen and 70% for renewable hydrogen will be used to calculate the total emissions according to the hydrogen share. Table 19 summarizes the total estimated demand in 2030 and 2050 for hydrogen production technology and the percentage for both reports.

Table 19. Shares of gray, blue, and green hydrogen in 2030 and 2050 demand. Own table based on Hydrogen Council (2021); IEA (2021b).

	International Energy Agency (IEA)							The Hydrogen Council (THC)						
Term (year)	Total (Mt)	Gray (Mt)	%	Blue (Mt)	%	Green (Mt)	%	Total (Mt)	Gray (Mt)	%	Blue (Mt)	%	Green (Mt)	%
2030	212	61.5	29	69.2	33	81.2	38	140	64.5	46	49.8	36	25.7	18
2050	528	10.5	2	196.6	37	320.8	61	660	0	0	198	30	462	70

The demand in 2020 and the expected hydrogen demand are presented in Figure 28 according to the estimates by the IEA and THC (Hydrogen Council, 2021; IEA, 2021b), adopting the demand in 2020 as a starting point which was 87 Mt of hydrogen (90% gray, 9.8% blue and 0.2% green)(IEA, 2021b, p. 76). In both scenarios, hydrogen demand will increase. The difference between the two estimates in 2030 is around 72 Mt, while in 2050 consists of 132 Mt, which could be considerable in terms of $CO_{2\text{-eq}}$ emissions. Figure 29 depicts the share of gray, blue, and green hydrogen in 2020, 2030, and 2050. The figure portrays that gray hydrogen slightly reduces its share from 2020 to 2030 to become almost insignificant by 2050. On the other hand, low-carbon hydrogen (blue and green) is expected to increase its stake to nearly 100% to reduce emissions.

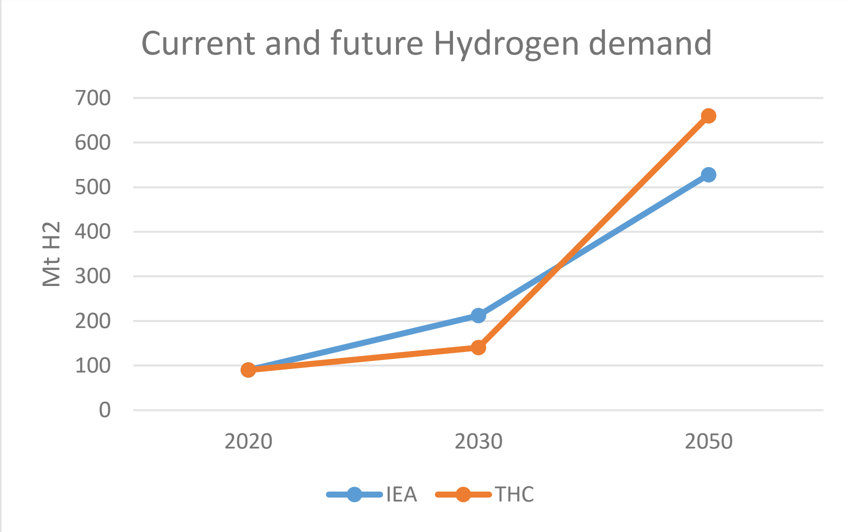

Figure 28. Hydrogen demand in 2020, 2030, and 2050 according to IEA and THC scenarios. Own figure based on Hydrogen Council (2021); IEA (2021b).

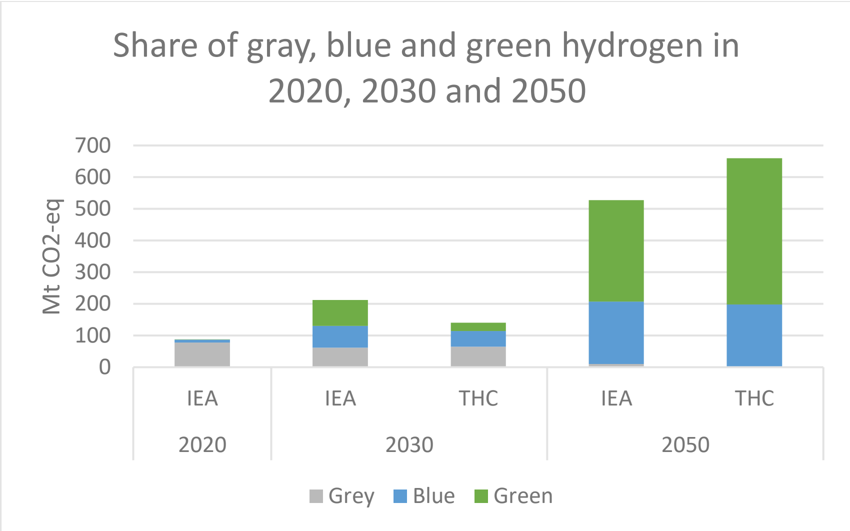

Figure 29. Share of gray, blue, and green hydrogen in 2020, 2030, and 2050 by IEA and THC. Own figure based on Hydrogen Council (2021); IEA (2021b).

These two demand estimates, and the respective share of every color of hydrogen, are used to calculate the $CO_{2\text{-eq}}$ emissions. The emissions from blue hydrogen in Table 16 and the emissions from green hydrogen in Table 17 are used.

5.3. Calculated $CO_{2\text{-eq}}$ Emissions for Hydrogen Demand in 2020

To compare future $CO_{2\text{-eq}}$ emissions of the future hydrogen demand, the possible $CO_{2\text{-eq}}$ emissions in 2020 from the reported hydrogen demand are calculated using the parameters mentioned in sections 5.1 and 5.2. The $CO_{2\text{-eq}}$ emissions in 2020 (yellow) were estimated using a carbon intensity on average of 9.7 kg $CO_{2\text{-eq}}$/kgH_2 (IEA, 2022c) and total demand of 87 Mt H_2; this scenario is referred to as 'IEA 2020'. As this estimate of 87 Mt H_2 does not specify which global warming potential was used, for this thesis, GWP20 and GWP100 are used to calculate $CO_{2\text{-eq}}$ emissions in 2020 and, thus, obtain a broader range of results for comparison.

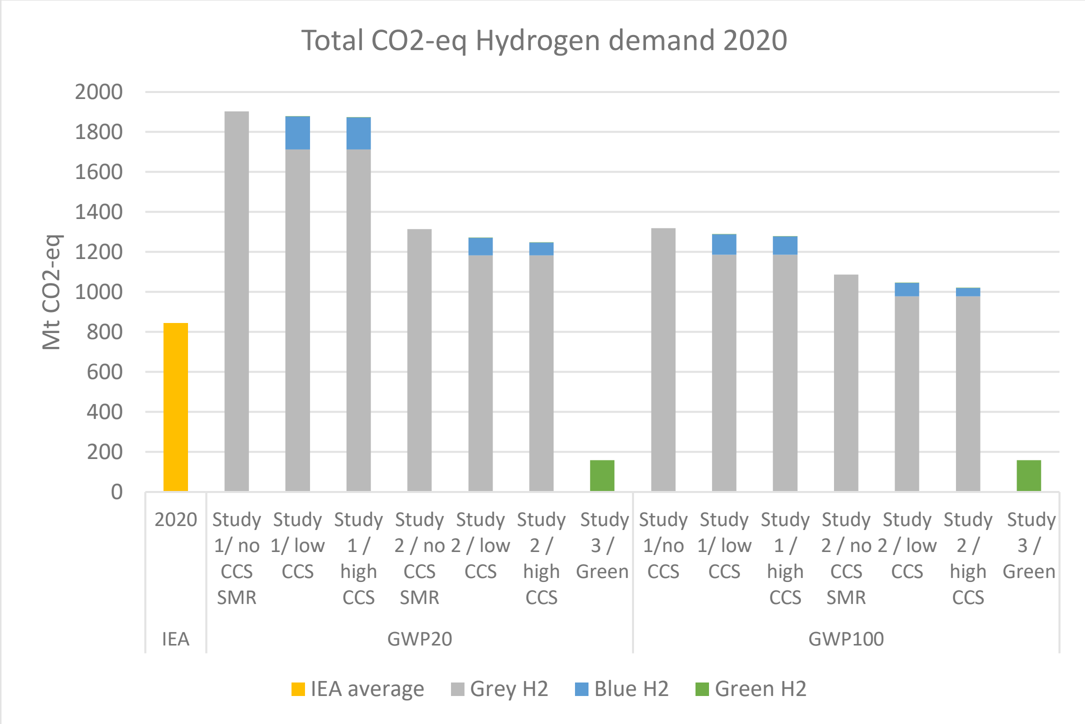

Figure 30. Total CO2-eq emissions from hydrogen demand in 2020. Own figure.

According to Figure 30, calculated emissions in 2020 with data from the ‘IEA 2020’ scenario were estimated to be around 844 Mt $CO_{2\text{-eq}}$ (yellow bar). Following this calculation, the same total hydrogen demand of 87 Mt and its share of gray (90%), blue (9.8%), and green (0.2%) were used to calculate the $CO_{2\text{-eq}}$ emissions for every scenario described in Table 16. The central figure shows an increase in emissions in every scenario, as gray hydrogen dominated the share in 2020. The only two scenarios showing the opposite trend are where total hydrogen demand had been produced from renewable sources.

Analyzing the results with a GWP20, emissions from ‘Study 1’ were more than doubled than the emissions from ‘IEA 2020’. Although ‘Study 2’ yields fewer emissions, they are high and are between 43-51% higher than the emissions from ‘IEA 2020’.

If $CO_{2\text{-eq}}$ is calculated using a GWP100, there is a considerable decrease in total emissions. However, ‘Study 1’ still yields 47 to 52% more emissions than ‘IEA 2020’ whereas ‘Study 2’ gets closer with a total of 1021 to 1088 Mt $CO_{2\text{-eq}}$ (though above) compared to the average estimate ‘IEA 2020’ of 844 Mt $CO_{2\text{-eq}}$.

The result of this calculation indicates what the trend is regarding emissions from the different hydrogen production methods. Furthermore, it is evident that the average carbon intensity estimated by the IEA is more conservative, which is a comparative point for the results presented in this thesis.

5.4. Calculated $CO_{2\text{-}eq}$ Emissions from Future Hydrogen Demand in 2030

Emissions from hydrogen demand in 2030 will be calculated following the previous steps in section 5.3. However, IEA and THC's estimated hydrogen demand in 2030 is different for this section. Therefore, every scenario will have its section. In this section, emissions will be calculated using GWP20 and GWP100. For comparison, 'IEA 2020' is calculated as in the previous section along with 'IEA 2030', which is the estimated demand by IEA in 2030 using as a carbon intensity an average of 4.5 kg $CO_{2\text{-}eq}/kgH_2$ (IEA, 2022c).

5.4.1 Scenario IEA 2030

Emissions in the IEA scenario are calculated using the data in Table 16 and estimated hydrogen demand by share of gray, blue, and green in Table 19. Figure 31 presents the results for this hydrogen demand of 212 Mt in 2030. The highest emissions come from the scenarios where gray hydrogen supplies 100% of the future demand. From this point, emissions start decreasing as the estimated share of low-carbon hydrogen is more than two-thirds of the total demand. However, in 'Study 1', there is almost the same amount of emissions from the gray and blue hydrogen, whereas in 'Study 2', gray hydrogen emits more $CO_{2\text{-}eq}$ despite the lower share. In both GWP, total emissions are more significant than the average presented in 'IEA 2030', which yields around 954 Mt $CO_{2\text{-}eq}$. It means an average carbon intensity of 4.5 $kgCO_{2\text{-}eq}/kgH_2$ could be an underestimation of emissions, as just the 'Study 2 / high CCS' could reduce the total emissions to 1,263 Mt $CO_{2\text{-}eq}$. This is 32% over the 'IEA 2030' estimation. If all the demand is supplied by green hydrogen in 'Study 3', total emissions would be around 388 Mt $CO_{2\text{-}eq}$. This is a 54% and 60% reduction compared to the emissions by 'IEA 2020' and 'IEA 2030', respectively.

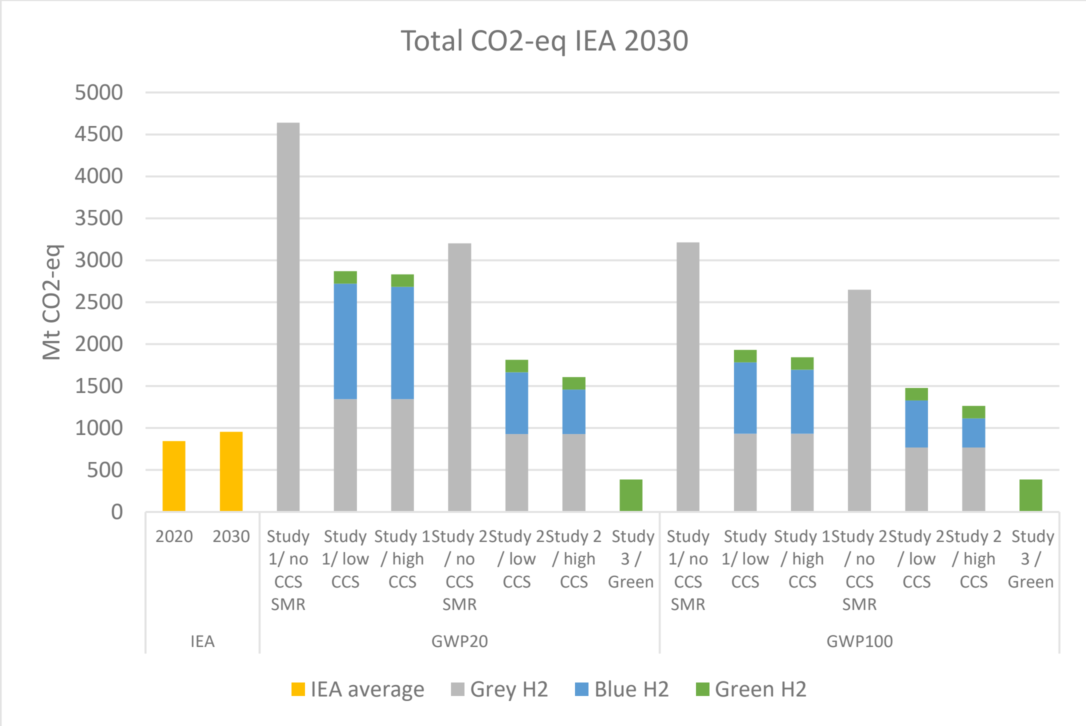

Figure 31. Total CO2-eq emissions from hydrogen demand by IEA in 2030. Own figure.

5.4.2 Scenario THC 2030

Emissions in the THC scenario are calculated using the data in Table 16 and estimated hydrogen demand by share of gray, blue, and green in Table 19. For this scenario, demand is expected to reach 140 Mt of hydrogen. It is a conservative number compared to the IEA estimate of 212 Mt. In Figure 32, emissions are the highest when the total demand comes from gray hydrogen in both GWP20 and GWP100. However, calculated $CO_{2\text{-eq}}$ emissions do not decline as expected when the share of gray, blue, and green hydrogen is considered. This is due to the large percentage of gray hydrogen, which is almost 50% of the total demand (compared to 29% in the IEA's estimate). Therefore, emissions from gray hydrogen represent the more significant portion in every scenario. Emissions from 'Study 2 / high CCS' are 1,102 Mt $CO_{2\text{-eq}}$, which is 75% over the 'IEA 2030', which was calculated with the THC estimate of 140 Mt H_2 and a carbon intensity average of 4.5 kg $CO_{2\text{-eq}}$/kgH_2 (IEA, 2022c). If all the demand were supplied by green hydrogen, emissions would be less than half of the one shown for 'IEA 2030'. Using a GWP100 yields fewer emissions. However, results show that it is far to reach a value close to 630 Mt $CO_{2\text{-eq}}$ with a hydrogen demand of 140 Mt H_2 in all scenarios, with the estimated share of gray, blue, and green by THC in 2030.

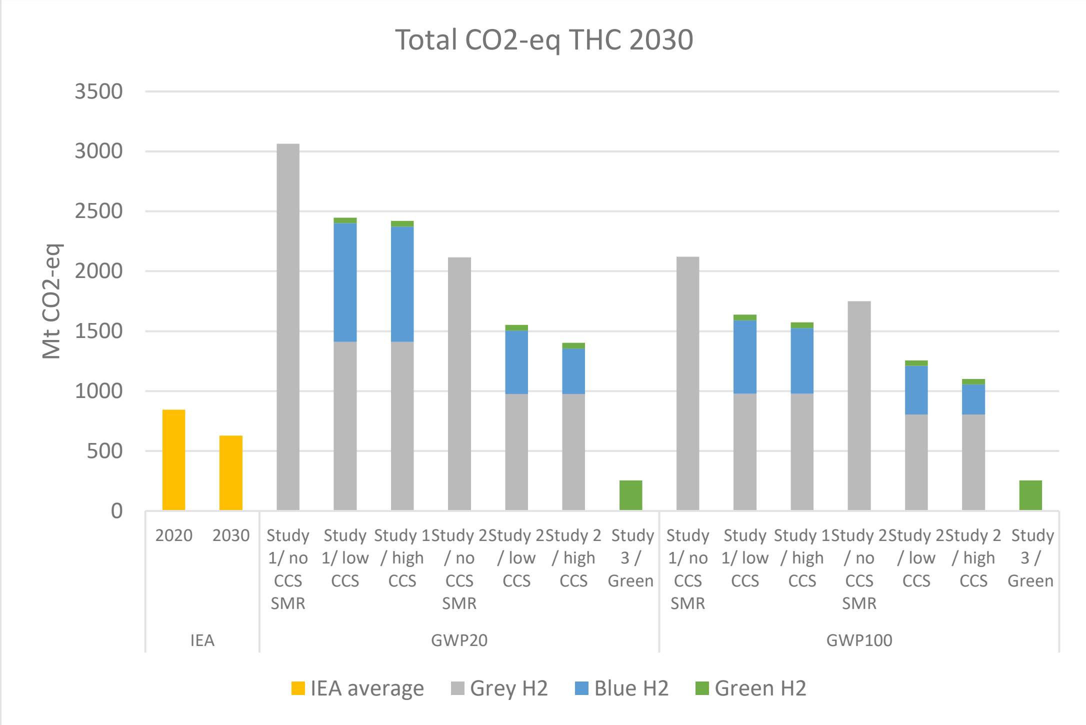

Figure 32. Total CO2-eq emissions from hydrogen demand by THC in 2030. Own figure.

5.5. Calculated $CO_{2\text{-eq}}$ Emissions from Future Hydrogen Demand in 2050

Emissions from hydrogen demand in 2050 will be calculated following the steps presented in section 5.4. First, the estimated hydrogen demand in 2050 by IEA and THC and the expected shares of gray, blue, and green hydrogen in these demands are used to calculate the $CO_{2\text{-eq}}$ emissions. The IEA and THC scenario will have their section where results will be given with a GWP20 and GWP100. The 'IEA 2050' uses the same expected carbon intensity of 4.5 kg $CO_{2\text{-eq}}$ /kgH_2 (IEA, 2022c), as there was no information for average carbon intensity in 2050. For comparison, 'IEA 2020' is calculated as in the previous section along with 'IEA 2030' to observe the short-term and long-term emissions trend.

5.5.1 Scenario IEA 2050

Emissions in the IEA scenario are calculated using for the year 2050 the data in Table 16 and estimated hydrogen demand by share of gray, blue, and green in Table 19. Figure 33 presents the results for this hydrogen demand of 528 Mt in 2050. A high number of emissions can be observed if all hydrogen demand were produced by gray hydrogen. This is, of course, due to the increase in demand for more than double from 2030 to 2050. When the share of gray, blue, and green is used to calculate emissions. Emissions decrease in more than half in 'Study 1' and

‘Study 2’ in both low and high CCS compared to 100% gray hydrogen, as gray hydrogen share is expected to be around 2%. In both GWP, total emissions, including ‘Study 3’ with 100% green hydrogen, are more significant than the emissions presented in ‘IEA 2030’, which yields around 954 Mt $CO_{2\text{-eq}}$. ‘Study 2 / high CCS presents less $CO_{2\text{-eq}}$ emissions per kg H_2 than ‘IEA 2050’, meaning that the average carbon intensity could be lower than 4.5 kg $CO_{2\text{-eq}}$ /kgH_2 (IEA, 2022c). If all the demand is supplied by green hydrogen, total emissions would be around 966 Mt $CO_{2\text{-eq}}$, the lowest in this scenario. Moreover, with ‘Study 3’, there is an increase of around 1% compared to the emissions from ‘IEA 2030’, which is insignificant in 20 years, and a hydrogen demand of more than doubled.

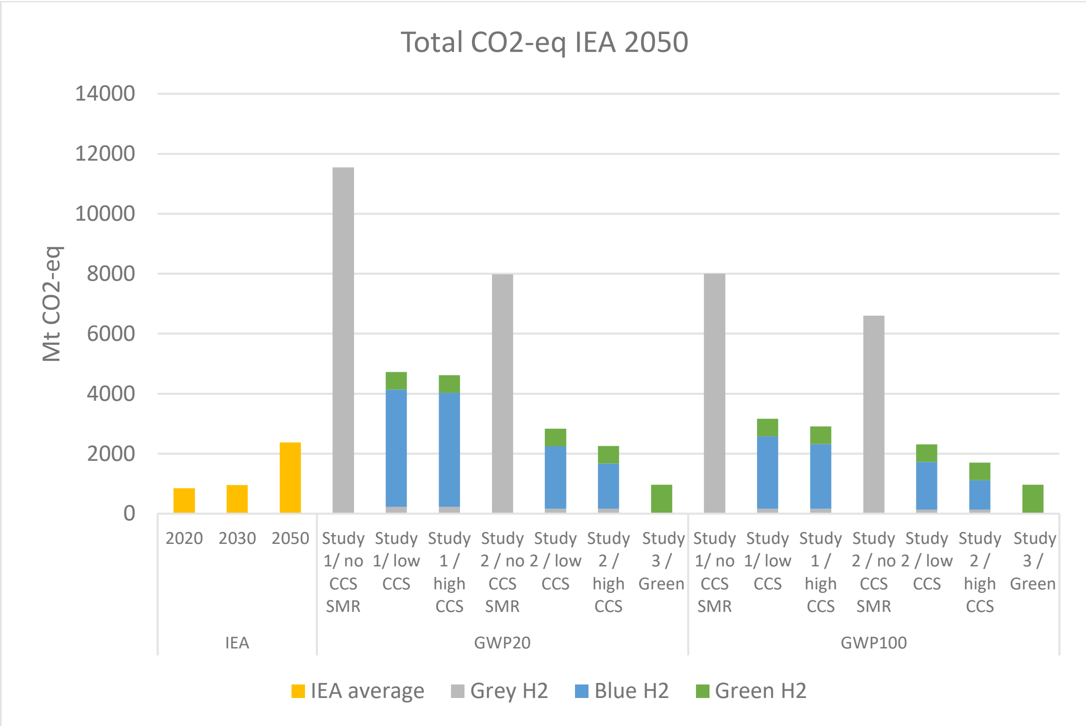

Figure 33. Total CO2-eq emissions from hydrogen demand by IEA in 2050. Own figure

5.5.2 Scenario THC 2050

Emissions in the THC scenario are calculated using the data in Table 16 and the estimated hydrogen demand of 660 Mt by share of gray, blue, and green in Table 19. Like the previous analysis, results were calculated and are presented in Figure 34. For this scenario, demand is expected to be 25% higher than the one from IEA in 2050 (section 5.5.1). However, $CO_{2\text{-eq}}$ emissions are just slightly higher. This is because the share of gray hydrogen in this scenario is expected to be zero (the one with the highest carbon intensity), and green and blue hydrogen are 70 and 30%, respectively. Therefore, if all demand was supplied by gray hydrogen in ‘Study 1 / no CCS’ and ‘Study 2 / no CCS’ in both GWP20 and GWP100, emissions are the highest yield, compared to the previous analysis in this thesis. Therefore, when calculating emissions in 'Study 1' with low and high CCS, the reduction in emissions is estimated to be around 68% (GWP20) and between 67-70% (GWP100). Whereas for 'Study 2' with low and high CCS, it is between 70-76% (GWP20) and 70-78% (GWP100). In the event of supplying the total demand with green hydrogen, emissions increased by around 20%, compared to 'IEA 2030' (180 Mt H_2).

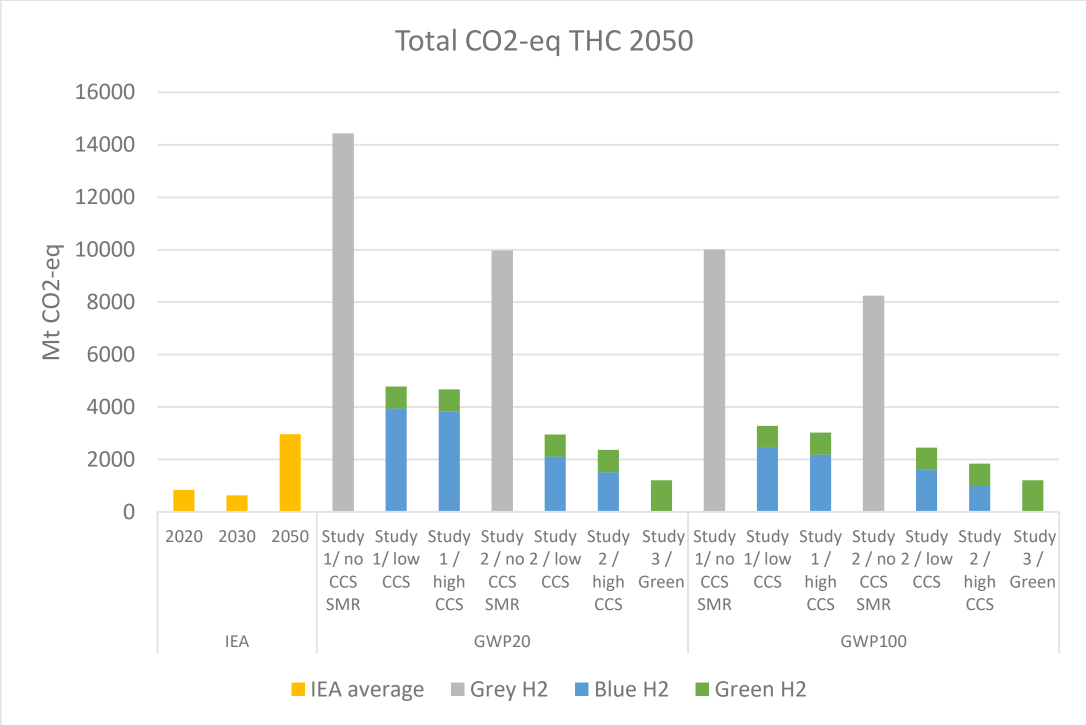

Figure 34. Total CO2-eq emissions from hydrogen demand by IEA in 2050. Own figure.

The 'IEA 2050' (yellow) is higher than the 'Study 2' configurations in both GWP20 and GWP100. However, 'Study 1' is higher than 'IEA 2050'. Therefore, if all hydrogen production were supplied by green hydrogen (Study 3), emissions would be 43% higher than the ones in IEA 2020 (30 years period) or slightly higher than emissions calculated for 2020 in section 5.3, which were between 1,021-1,290 Mt H_2 with GWP20 and 1,247-1,879 Mt H_2 with GWP20.

5.6. Calculated $CO_{2\text{-eq}}$ Emissions from Future Hydrogen Demand for 'Study 4'.

Emissions from 'Study 4' are separated from the previous analysis, as the conditions in which the carbon intensity was calculated differ from the previous ones. As a result, this study yields the lowest carbon intensity in kg $CO_{2\text{-eq}}$ /kgH_2. In 'Study 4', natural gas and hydrogen transport distance plays an important role. It is based on importing hydrogen instead of natural gas to minimize methane leakage and its use.

As explained in section 4.2, natural gas is transported to a maximum distance of 300 km by a pipeline and converted to blue hydrogen. Then, it is exported through a 4000 km pipeline to be used (Schippert et al., 2022). Due to the lower carbon intensity, it is worth calculating the total $CO_{2\text{-eq}}$ emission of it in this thesis.

For this scenario, 'Study 1' is left out, as it does not consider the specific distance parameter mentioned above. Hence, the comparison only considers 'Study 2' and the estimated demand for 2030 and 2050 for both IEA and THC scenarios. Data was taken from Table 16 and Table 19. As 'Study 1' was not considered, $CO_{2\text{-eq}}$ emissions from the estimated demand for both IEA and THC are compiled with a global warming potential of GWP20 and GWP100. Results for the short-term (2030) and the long-term (2050) are presented in different sections. Emissions in 2020 and 2030 (yellow) were estimated using a carbon intensity on average of 9.7 and 4.5 kg $CO_{2\text{-eq}}$ / kgH_2, respectively.

5.6.1 Scenario 2030 IEA and THC

In the short term (see Figure 35), estimated hydrogen demand of 212 Mt (IEA) and 140 Mt (THC) would have a range of emission between 1181-1384 Mt $CO_{2\text{-eq}}$ in the low CCS scenario for 'Study 1' and 'Study 2', and 1017-1156 Mt $CO_{2\text{-eq}}$ in the high CCS scenario with GWP20. Using a GWP100 and IEA demand, the emissions in the 'Study 2 / high CCS' decrease to an extent in which emissions are just 13% higher than those from the 'IEA 2030' scenario.

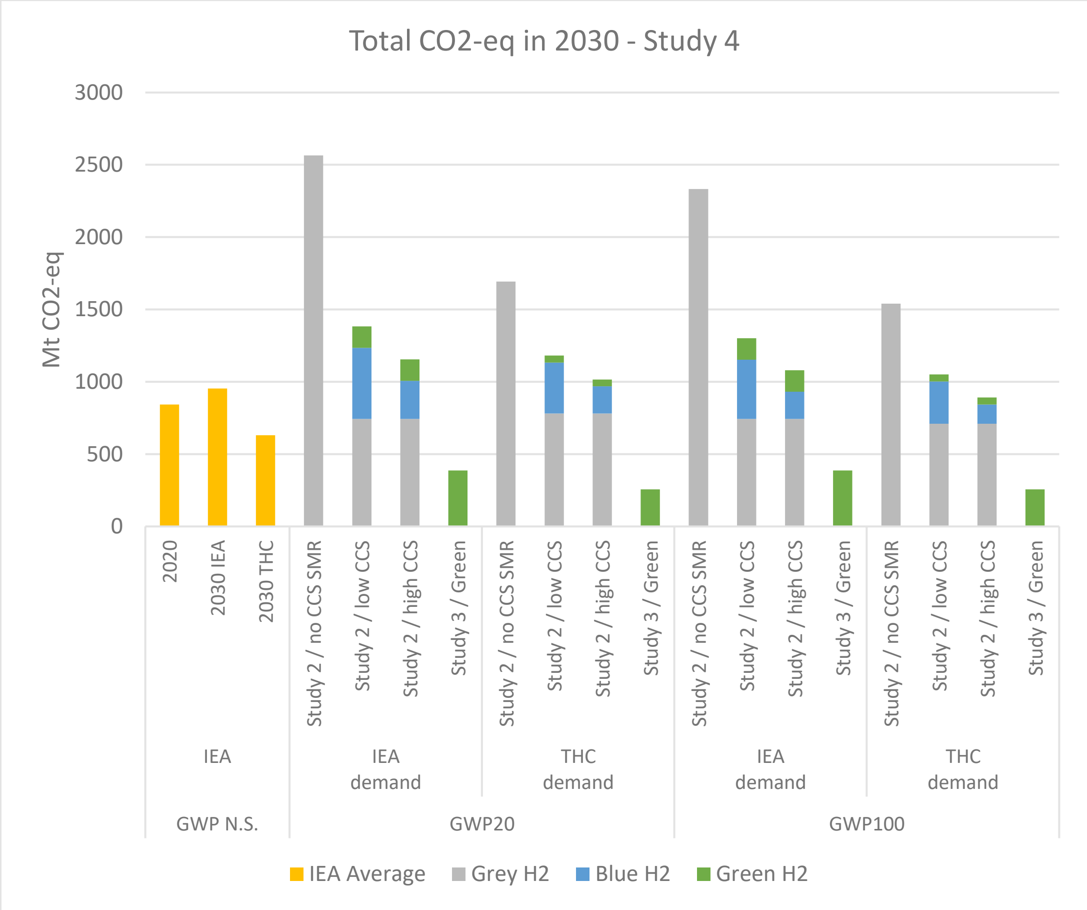

Figure 35. Total CO2-eq emissions in ‘Study 4’ from hydrogen demand by IEA and THC in 2030. Own figure.

To better observe the results, the option of producing 100% gray hydrogen was removed in Figure 36. It is evident that gray hydrogen still plays an important role in every scenario in 2030. Reducing the share of gray hydrogen in 2030 could reduce emissions close to the ‘IEA 2030’ scenarios. Achieving 100% of green hydrogen would reduce $CO_{2\text{-eq}}$ emissions by more than half compared to the ‘IEA 2030’ scenarios. Emissions would be even lower than those calculated in the ‘IEA 2020’ scenario, achieving an emissions reduction in ten years.

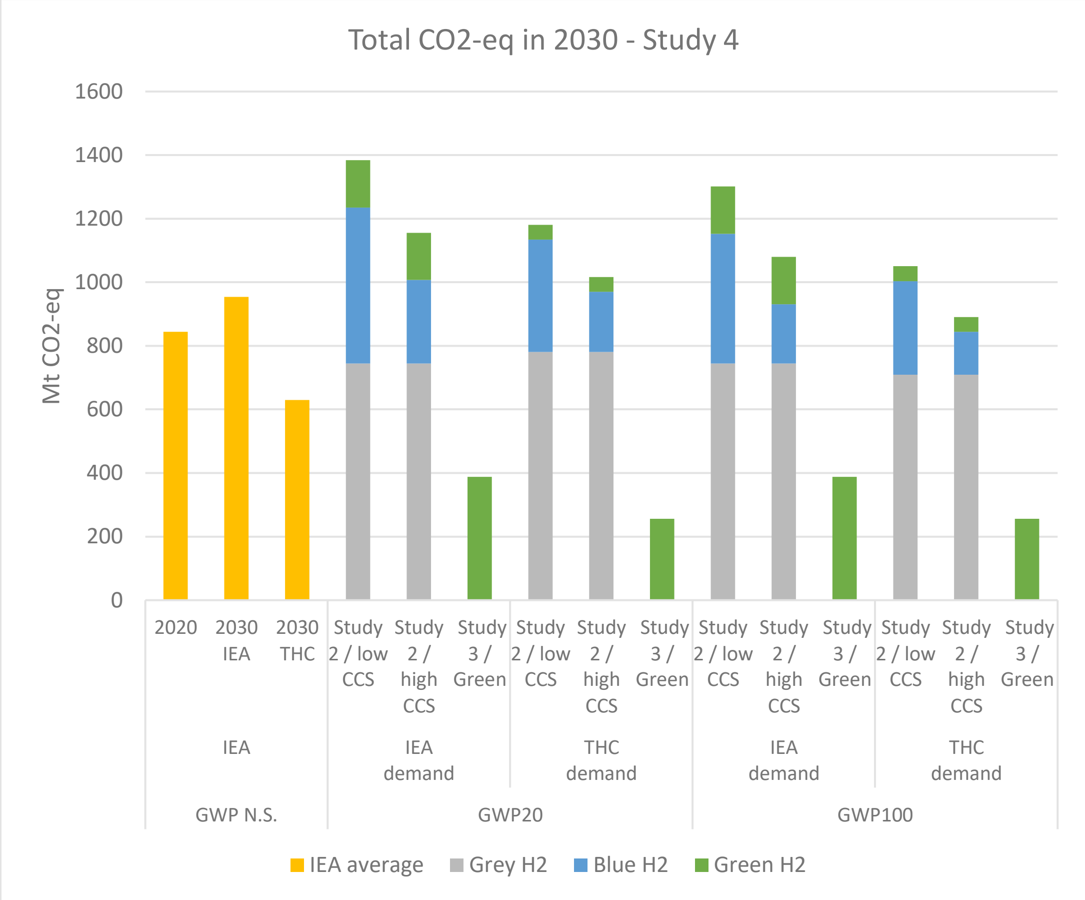

Figure 36. Total CO2-eq emissions in 'Study 4' from hydrogen demand by IEA and THC in 2030. There is no 100% gray hydrogen option. Own figure.

5.6.2 Scenario 2050 IEA and THC

For the 2050 scenario, the results of $CO_{2\text{-eq}}$ emissions are presented in Figure 37. The estimated hydrogen demand of 528 Mt (IEA) and 660 Mt (THC) would have a range of emission between 1874-2110 Mt $CO_{2\text{-eq}}$ in the low CCS scenario (Study 1 and Study 2) and 1245-1461 Mt $CO_{2\text{-eq}}$ in the high CCS scenario with GWP20. These high results come due to the increase in hydrogen demand by 2050. However, emissions are below 3000 Mt $CO_{2\text{-eq}}$ emissions marks, compared to results in section 5.5. Using a GWP100, all the scenarios go almost below the 2,000 Mt $CO_{2\text{-eq}}$ emissions mark.

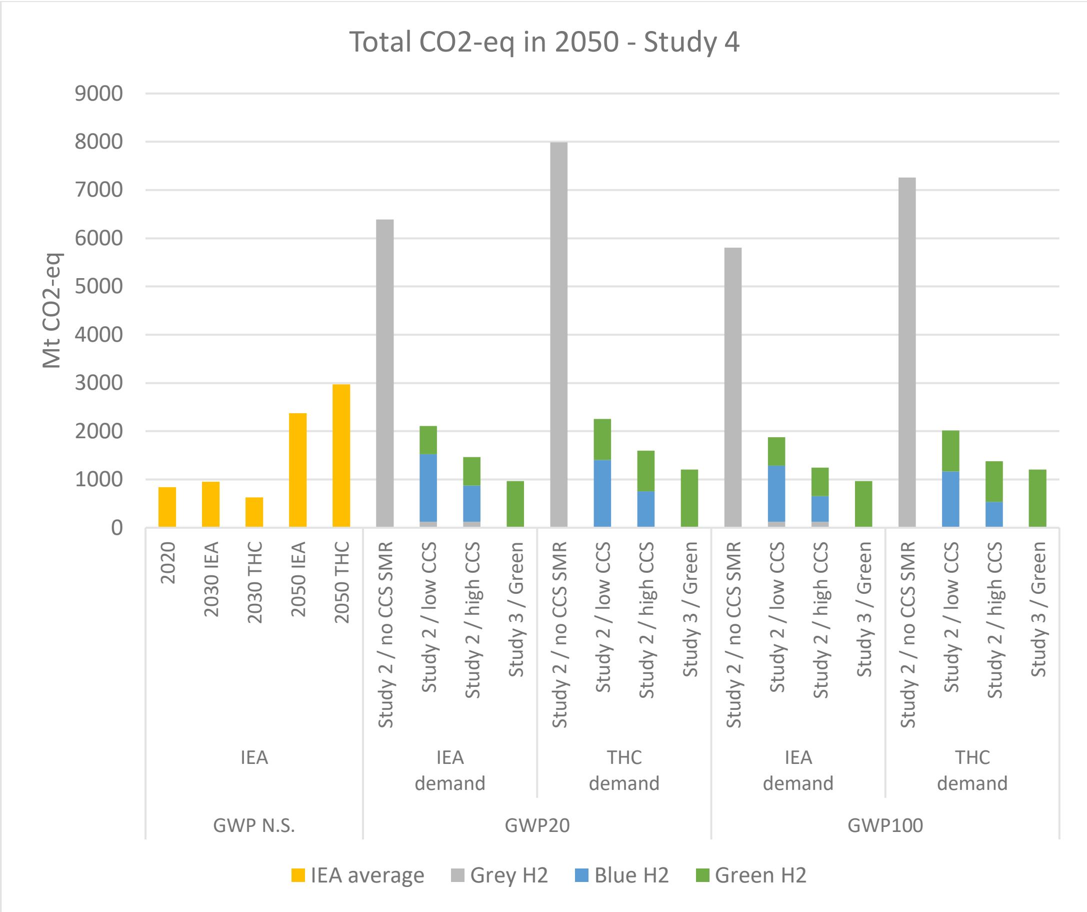

Figure 37. Total CO2-eq emissions in 'Study 4' from hydrogen demand by IEA and THC in 2050. Own figure.

As in the 2030 scenario, the scenarios where 100% gray hydrogen is produced were removed in Figure 38. By 2050, gray hydrogen will stop playing an important role, and its share will be reduced to 0-2%. However, all the scenarios are over the estimates of 'IEA 2020' and 'IEA 2030' as emissions are likely to increase with the increase in demand. Achieving 100% of green hydrogen would go slightly over the $CO_{2\text{-eq}}$ emissions from those in the 'IEA 2030' scenario and are the only ones yielding less emission in 2050 for both scenarios.

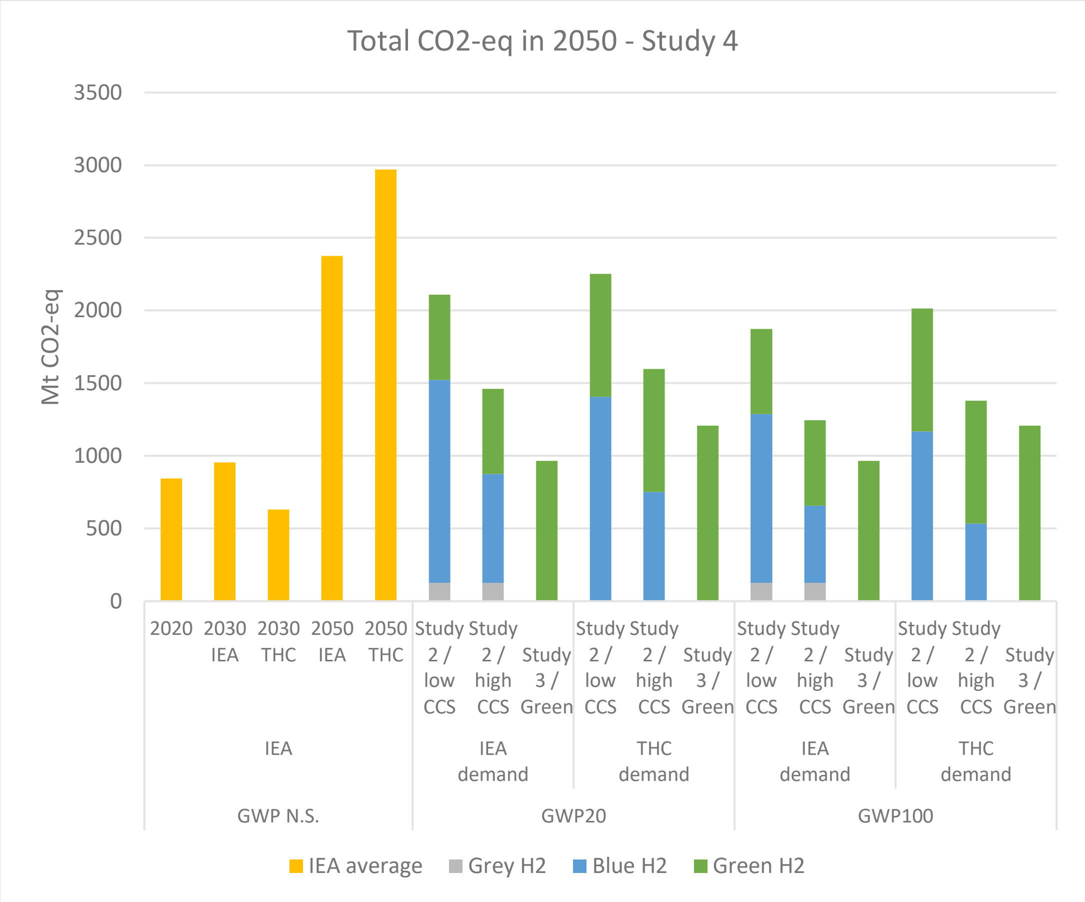

Figure 38 Total CO2-eq emissions in ‘Study 4’ from hydrogen demand by IEA and THC in 2050. There is no option for 100% gray hydrogen. Own figure.

Average carbon intensity using the values in ‘Study 4’ can be lower than the estimate of 9.7 in 2020 and 4.5 kg $CO_{2\text{-eq}}$ /kgH_2 in 2030 (IEA, 2022c). However, emissions from low CCS will almost double from 2020 to 2050. On the other hand, green hydrogen production will reduce emissions significantly compared to 2020 and 2030, as the future demand is expected to be more than five to six times higher.

6 Conclusion

Hydrogen is expected to play an essential role in reducing CO_2 emissions in the short and long term. This is because hydrogen has great potential to replace unabated fossil fuels in industry, transport, and energy sectors worldwide. According to estimates, hydrogen demand will increase by more than six times by 2050, and the mix of gray, blue, and green is one pillar to reduce $CO_{2\text{-eq}}$ emissions.

The selection of two studies with their respective carbon intensities and results reported in this thesis showed that $CO_{2\text{-eq}}$ emissions were underestimated in 2020, 2030 and possibly 2050, according to the current technological development. Additionally, carbon intensities in kg $CO_{2\text{-eq}}$/kgH_2 from gray, blue, and green hydrogen vary from every author according to their models, stages, and assumptions. Total emissions depend on the demand, the share of gray, blue, and green hydrogen, location, methane leakage, and the selection of global warming potential, which define the carbon intensity of hydrogen. It was found that there is no general standard yet among the selected authors for calculating $CO_{2\text{-eq}}$ emissions for hydrogen production.

In a world seeking to reduce emissions, priority must be given to low-emission technologies. However, blue hydrogen from low CCS shows high emissions in 2050 compared to 2020. Projects achieving high CCS could be developed where methane leakage and CCS rate are defined and controlled. In this thesis, it was shown that emissions from blue hydrogen with high CCS scenarios are close to the estimate by the IEA 2030. However, these scenarios are the best case in every model and, thus, do not represent what is currently achieved in terms of efficiency, carbon capture rate, and methane leakage.

Developed countries importing hydrogen from developing countries could help support initiatives and set up strict measurements for $CO_{2\text{-eq}}$ emission. This is important to ensure strict control of emission reductions. For example, national strategies might use average carbon intensities that do not correspond to accurate estimates. This could lead to an underestimation of total emissions.

Moreover, hydrogen production and its emissions must be assessed for each case independently and using average values can give inaccurate results. Implementation of hydrogen projects needs to be done per site, region, and country because not all countries have the same CH_4 emissions when producing or importing natural gas. The analysis in this thesis showed that the share of blue hydrogen could produce fewer emissions when the natural gas transport distance is shorter. Therefore, promoting blue hydrogen production in countries with natural gas could help achieve lower emissions, especially if the power plant is close to the oil fields and ports. However, additional emissions and energy to transport blue hydrogen overseas must be calculated and included.

Under the assumption that current conditions of producing and transporting natural gas do not change to mitigate methane leakage, blue hydrogen could have higher $CO_{2\text{-eq}}$ emissions in 2030 and 2050 than in 2020, as it is expected to increase its share by around 30%. Furthermore, gas and oil prices are volatile. Their prices decreased during 2020 because of the Covid pandemic. However, they increased rapidly due to the Russian war in Ukraine. It reflects how fossil fuel prices can affect the further deployment and performance of blue hydrogen.

Green hydrogen is the best option to obtain the lowest levels of CO_2 emissions compared to blue and gray hydrogen. However, it depends on the technology adopted and the carbon intensity. This thesis used a calculated average value of 1.83 $KgCO_{2\text{-eq}}$/ kgH_2 for green hydrogen via electrolysis using Solar PV and wind electricity. The analysis showed that the higher the carbon intensity for green hydrogen, the higher the $CO_{2\text{-eq}}$ emissions. Most importantly, the main goal for developing hydrogen is its contribution to reducing $CO_{2\text{-eq}}$ emissions. Thus, priority must be given to hydrogen technology with fewer emissions, which is green hydrogen production via water electrolysis. Moreover, costs for green hydrogen tend to decrease in the long term, gaining parity with blue hydrogen. The development of renewable infrastructure is complementary and will help to deploy green hydrogen.

In conclusion, comparing blue with gray hydrogen production, there is a reduction of $CO_{2\text{-eq}}$ emissions. However, these emissions need to be accurately measured, and as a result, different values depending on the approach are calculated. This causes uncertainty regarding the estimation of future emissions and may lead to misleading decisions. Green hydrogen via water electrolysis demonstrated low $CO_{2\text{-eq}}$ emissions as there is no direct use of fossil fuels.

For further work, green and blue hydrogen technologies should be assessed in economic terms, considering the costs of non-action, the risks included by a further increase of emissions, and the difficulty of anticipating the effects of climate change. In addition, other hydrogen production methods, such as SMR from biomass and methane pyrolysis, are worth evaluating to add more options to the low-carbon hydrogen mix.

Bibliography

Admin, L. (2019, March). What is the difference between the “higher heating value” (HHV) and “lower heating value” (LHV) of a biomass fuel, and why is the difference important? – Livestock and Poultry Environmental Learning Community. Livestock and Poultry Environmental Learning Community. https://lpelc.org/what-is-the-difference-between-the-higher-heating-value-hhv-and-lower-heating-value-lhv-of-a-biomass-fuel-and-why-is-the-difference-important/

Air Liquide. (2021, January 26). Air Liquide inaugurates the world’s largest low-carbon hydrogen membrane-based production unit in Canada. Air Liquide. https://www.airliquide.com/group/press-releases-news/2021-01-26/air-liquide-inaugurates-worlds-largest-low-carbon-hydrogen-membrane-based-production-unit-canada

Antonini, C., Treyer, K., Streb, A., van der Spek, M., Bauer, C., & Mazzotti, M. (2020). Hydrogen production from natural gas and biomethane with carbon capture and storage – A techno-environmental analysis. Sustainable Energy & Fuels, 4(6), 2967–2986. https://doi.org/10.1039/D0SE00222D

Arat, H., & Sürer, M. (2018). State of art of hydrogen usage as a fuel on aviation. European Mechanical Science, 2, 20–30. https://doi.org/10.26701/ems.364286

Bandilla, K. W. (2020). 31—Carbon Capture and Storage. In T. M. Letcher (Ed.), Future Energy (Third Edition) (pp. 669–692). Elsevier. https://doi.org/10.1016/B978-0-08-102886-5.00031-1

Basile, A., Subramani, V., & Veziroglu, T. N. (2015). Compendium of hydrogen energy.: (Hydrogen production and purification) (Vol. 83, Issue ISBN: 9781782423614). Woodhead Publishing.

Bauer, C., Treyer, K., Antonini, C., Bergerson, J., Gazzani, M., Gencer, E., Gibbins, J., Mazzotti, M., McCoy, S. T., McKenna, R., Pietzcker, R., Ravikumar, A. P., Romano, M. C., Ueckerdt, F., Vente, J., & van der Spek, M. (2022). On the climate impacts of blue hydrogen production. Sustainable Energy & Fuels, 6(1), 66–75. https://doi.org/10.1039/D1SE01508G. License: CC BY 3.0.

Braga, L. B., da Silva, M. E., Colombaroli, T. S., Tuna, C. E., de Araujo, F. H. M., Vane, L. F., Pedroso, D. T., & Silveira, J. L. (2017a). Hydrogen Production Processes. In J. L. Silveira (Ed.), Sustainable Hydrogen Production Processes (pp. 5–76). Springer International Publishing. https://doi.org/10.1007/978-3-319-41616-8_2

Braga, L. B., Tuna, C. E., de Araujo, F. H. M., Vane, L. F., Pedroso, D. T., & Silveira, J. L. (2017b). Economic Studies of Some Hydrogen Production Processes. In J. L. Silveira (Ed.), Sustainable Hydrogen Production Processes (pp. 109–125). Springer International Publishing. https://doi.org/10.1007/978-3-319-41616-8_4

Chen, S., Liu, J., Zhang, Q., Teng, F., & McLellan, B. C. (2022). A critical review on deployment planning and risk analysis of carbon capture, utilization, and storage (CCUS) toward carbon neutrality. Renewable and Sustainable Energy Reviews, 167, 112537. https://doi.org/10.1016/j.rser.2022.112537

Engineering ToolBox. (2003). Fuels—Higher and Lower Calorific Values. Engineering ToolBox. https://www.engineeringtoolbox.com/fuels-higher-calorific-values-d_169.html

Espegren, K., Damman, S., Pisciella, P., Graabak, I., & Tomasgard, A. (2021). The role of hydrogen in the transition from a petroleum economy to a low-carbon society. International Journal of Hydrogen Energy, 46(45), 23125–23138. https://doi.org/10.1016/j.ijhydene.2021.04.143

Global CCS Institute. (2021). The Global Status of CCS: 2021. ©Global Carbon Capture and Storage Institute Ltd 2021.

Gonzalez-Diaz, A., Jiang, L., Gonzalez-Diaz, M. O., Roskilly, A. P., & Smallbone, A. J. (2021). Hydrogen production via ammonia from methane integrated with enhanced oil recovery: A techno-economic analysis. Journal of Environmental Chemical Engineering, 9(2), 105050. https://doi.org/10.1016/j.jece.2021.105050

Guo, Y., Li, G., Zhou, J., & Liu, Y. (2019). Comparison between hydrogen production by alkaline water electrolysis and hydrogen production by PEM electrolysis. IOP Conference Series: Earth and Environmental Science, 371(4), 042022. https://doi.org/10.1088/1755-1315/371/4/042022

Howarth, R. W., & Jacobson, M. Z. (2021). How green is blue hydrogen? Energy Science & Engineering, 9(10), 1676–1687. https://doi.org/10.1002/ese3.956. License: CC BY 4.0.

Hydrogen Council. (2021). Hydrogen for Net-Zero: A critical cost-competitive energy vector.

IEA. (2019). The Future of Hydrogen. IEA, Paris. https://www.iea.org/reports/the-future-of-hydrogen. License: CC BY 4.0.

IEA. (2020). Energy Technology Perspectives 2020. IEA, Paris. https://www.iea.org/reports/energy-technology-perspectives-2020. License: CC BY 4.0.

IEA. (2021a). Global Hydrogen Review 2021. IEA, Paris. https://www.iea.org/reports/global-hydrogen-review-2021. License: CC BY 4.0.

IEA. (2021b). Net Zero by 2050. IEA, Paris. https://www.iea.org/reports/net-zero-by-2050. License: CC BY 4.0.

IEA. (2022a). Clean Energy Demonstration Projects Database. IEA, Paris. https://www.iea.org/data-and-statistics/data-tools/clean-energy-demonstration-projects-database?status=Operational&subsector=Hydrogen

IEA. (2022b). Hydrogen. IEA, Paris. https://www.iea.org/reports/hydrogen. License: CC BY 4.0.

IEA. (2022c). Hydrogen Supply. IEA, Paris. https://www.iea.org/reports/hydrogen-supply. License: CC BY 4.0.

IPCC. (2022). Global Warming of 1.5°C: IPCC Special Report on impacts of global warming of 1.5°C above pre-industrial levels in context of strengthening response to climate change, sustainable development, and efforts to eradicate poverty (1st ed.). Cambridge University Press. https://doi.org/10.1017/9781009157940

IRENA. (2018). Hydrogen from renewable power: Technology outlook for the energy transition. International Renewable Energy Agency, Abu Dhabi.

IRENA. (2020a). Green Hydrogen: A guide to policy making. International Renewable Energy Agency, Abu Dhabi.

IRENA. (2020b). Green Hydrogen cost reduction: Scaling up electrolysers to meet the 1.5 C goal. International Renewable Energy Agency, Abu Dhabi.

IRENA. (2022a). Global hydrogen trade to meet the 1.5°C climate goal: Part I – Trade outlook for 2050 and way forward. International Renewable Energy Agency, Abu Dhabi.

IRENA. (2022b). World Energy Transitions Outlook 2022: 1.5°C Pathway. International Renewable Energy Agency, Abu Dhabi.

Johnston, D. M., Sefcik, S. E., & Soderstrom, N. S. (2008). The Value Relevance of Greenhouse Gas Emissions Allowances: An Exploratory Study in the Related United States SO2 Market. European Accounting Review, 17(4), 747–764. https://doi.org/10.1080/09638180802481615

Kumar, A., Nagar, S., & Anand, S. (2021). 1—Climate change and existential threats. In S. Singh, P. Singh, S. Rangabhashiyam, & K. K. Srivastava (Eds.), Global Climate Change (pp. 1–31). Elsevier. https://doi.org/10.1016/B978-0-12-822928-6.00005-8

Lamb, J. J., Hillestad, M., Rytter, E., Bock, R., Nordgård, A. S. R., Lien, K. M., Burheim, O. S., & Pollet, B. G. (2020). Chapter | three—Traditional Routes for Hydrogen Production and Carbon Conversion. In J. J. Lamb & B. G. Pollet (Eds.), Hydrogen, Biomass and Bioenergy (pp. 21–53). Academic Press. https://doi.org/10.1016/B978-0-08-102629-8.00003-7

Lamb, Wiedmann, T., Pongratz, J., Andrew, R., Crippa, M., Olivier, J., Wiedenhofer, D., Mattioli, G., Al Khourdajie, A., House, J., Pachauri, S., Figueroa, M., Saheb, Y., Slade, R., Klaus, H., Sun, L., Ribeiro, S., Khennas, S., Can, S., & Minx, J. (2021). A review of trends and drivers of greenhouse gas emissions by sector from 1990 to 2018. Environmental Research Letters, 16. https://doi.org/10.1088/1748-9326/abee4e. License: CC BY 4.0.

Longden, T., Beck, F. J., Jotzo, F., Andrews, R., & Prasad, M. (2022). 'Clean' hydrogen? – Comparing the emissions and costs of fossil fuel versus renewable electricity based hydrogen. Applied Energy, 306, 118145. https://doi.org/10.1016/j.apenergy.2021.118145

Mazloomi, K., & Gomes, C. (2012). Hydrogen as an energy carrier: Prospects and challenges. Renewable and Sustainable Energy Reviews, 16(5), 3024–3033. https://doi.org/10.1016/j.rser.2012.02.028

Ministerio de Minas y Energía. (2021). Hoja de Ruta de Hidrógeno de Colombia. https://www.minenergia.gov.co/static/ruta-hidrogeno/src/document/Hoja%20Ruta%20Hidrogeno%20Colombia_2810.pdf

NASA. (2022, January). 2021 Tied for 6th Warmest Year in Continued Trend, NASA Analysis Shows. NASA Climate Change: Vital Signs of the Planet. https://climate.nasa.gov/news/3140/2021-tied-for-6th-warmest-year-in-continued-trend-nasa-analysis-shows

Nikolaidis, P., & Poullikkas, A. (2017). A comparative overview of hydrogen production processes. Renewable and Sustainable Energy Reviews, 67, 597–611. https://doi.org/10.1016/j.rser.2016.09.044

Noussan, M., Raimondi, P. P., Scita, R., & Hafner, M. (2020). The Role of Green and Blue Hydrogen in the Energy Transition—A Technological and Geopolitical Perspective. Sustainability, 13(1), 298. https://doi.org/10.3390/su13010298

Palmer, G., Roberts, A., Hoadley, A., Dargaville, R., & Honnery, D. (2021). Life-cycle greenhouse gas emissions and net energy assessment of large-scale hydrogen production via electrolysis and solar PV. Energy & Environmental Science, 14(10), 5113–5131. https://doi.org/10.1039/D1EE01288F

Patel, S. (2022, July 1). Fukushima Hydrogen Energy Research Field Demonstrates Hydrogen Integration. POWER Magazine. https://www.powermag.com/fukushima-hydrogen-energy-research-field-demonstrates-hydrogen-integration/

REFHYNE. (2022). Project Overview. REFHYNE Clean Refinery Hydrogen for Europe. https://www.refhyne.eu/about/

Rock, L., O'Brien, S., Tessarolo, S., Duer, J., Bacci, V. O., Hirst, B., Randell, D., Helmy, M., Blackmore, J., Duong, C., Halladay, A., Smith, N., Dixit, T., Kassam, S., & Yaychuk, M. (2017). The Quest CCS Project: 1st Year Review Post Start of Injection. Energy Procedia, 114, 5320–5328. https://doi.org/10.1016/j.egypro.2017.03.1654

Schippert, J., Runge, P., Farhang-Damghani, N., & Grimm, V. (2022). Greenhouse Gas Footprint of Blue Hydrogen with Different Production Technologies and Logistics Options. SSRN Electronic Journal. https://doi.org/10.2139/ssrn.4153724

Shiva Kumar, S., & Himabindu, V. (2019). Hydrogen production by PEM water electrolysis – A review. Materials Science for Energy Technologies, 2(3), 442–454. https://doi.org/10.1016/j.mset.2019.03.002

Sovacool, B. K., Griffiths, S., Kim, J., & Bazilian, M. (2021). Climate change and industrial F-gases: A critical and systematic review of developments, sociotechnical systems and policy options for reducing synthetic greenhouse gas emissions. Renewable and Sustainable Energy Reviews, 141, 110759. https://doi.org/10.1016/j.rser.2021.110759

Speight, J. G. (2014). Chapter 5—The Fischer−Tropsch Process. In J. G. Speight (Ed.), Gasification of Unconventional Feedstocks (pp. 118–134). Gulf Professional Publishing. https://doi.org/10.1016/B978-0-12-799911-1.00005-4

Speight, J. G. (2019). Chapter 15—Hydrogen Production. In J. G. Speight (Ed.), Heavy Oil Recovery and Upgrading (pp. 657–697). Gulf Professional Publishing. https://doi.org/10.1016/B978-0-12-813025-4.00015-5

Suda, R. (2021, March 11). Fukushima's hydrogen potential lures Japan's car sector. Argus Media. https://www.argusmedia.com/en/news/2194885-fukushimas-hydrogen-potential-lures-japans-car-sector

UNFCCC. (2022). The Paris Agreement. United Nations Climate Change. https://unfccc.int/process-and-meetings/the-paris-agreement/the-paris-agreement

Valente, A., Iribarren, D., & Dufour, J. (2017). Harmonised life-cycle global warming impact of renewable hydrogen. Journal of Cleaner Production, 149, 762–772. https://doi.org/10.1016/j.jclepro.2017.02.163

Vincent, I., & Bessarabov, D. (2018). Low cost hydrogen production by anion exchange membrane electrolysis: A review. Renewable and Sustainable Energy Reviews, 81, 1690–1704. https://doi.org/10.1016/j.rser.2017.05.258

Yoro, K. O., & Daramola, M. O. (2020). Chapter 1—CO2 emission sources, greenhouse gases, and the global warming effect. In M. R. Rahimpour, M. Farsi, & M. A. Makarem (Eds.), Advances in Carbon Capture (pp. 3–28). Woodhead Publishing. https://doi.org/10.1016/B978-0-12-819657-1.00001-3

Yusaf, T., Laimon, M., Alrefae, W., Kadirgama, K., Dhahad, H. A., Ramasamy, D., Kamarulzaman, M. K., & Yousif, B. (2022). Hydrogen Energy Demand Growth Prediction and Assessment (2021–2050) Using a System Thinking and System Dynamics Approach. Applied Sciences, 12(2), 781. https://doi.org/10.3390/app12020781. License: CC BY 4.0.

Zohuri, B. (2019). Hydrogen Energy: Challenges and Solutions for a Cleaner Future (1st ed. 2019). Springer International Publishing : Imprint: Springer. https://doi.org/10.1007/978-3-319-93461-7

List of Abbreviations

AEL	Alkaline electrolyzer
AEM	Anion exchange membrane
AEMEL	Anion exchange membrane electrolysis
ATR	Autothermal reforming
CCS	Carbon capture and storage
CCUS	Carbon capture utilizations and storage
CG	Coal gasification
DRI	Direct reduced iron
EOR	Enhanced oil recovery
GHG	Greenhouse gas
GJ	Gigajoules
GWP	Global warming potential
HHV	Higher heating value
HTEL	High temperature electrolysis
LCA	Life cycle assessment
LCIA	Life cycle impact assessment
LHV	Lowe heating value
MEA	Monoethanolamide
MJ	Megajoules
Mt	Million tons
MW	Megawatt
NDC	National determined contribution
NG	Natural gas
PEM	Proton exchange membrane
PM	Particulate matter
POX	Partial oxidation
PV	Photovoltaic
R&D	Research and development
SMR	Steam methane reforming
SOEC	Solid oxide electrolyzer cell
SOEL	Solid oxide electrolyte electrolysis
SPE	Solid polymer electrolyte

SR	Steam reforming
VPSA	Vacuum pressure adsorption
WGS	Water-gas shift

List of Figures

List of Tables